TECHNICAL REPORT STANDARD PAGE

1. Report No. FHWA/LA.03/374	2. Government Accession No. 3. Recipient's Catalog No.
4. Title and Subtitle Comparative Performance of Rubber Modified Hot Mix Asphalt Under ALF Loading	5. Report Date August 2003 6. Performing Organization Code
7. Author(s) Freddy L. Roberts[1], Louay N. Mohammad[2], Hanlin Qin[1], Baoshan Huang[2]	8. Performing Organization Report No.
9. Performing Organization Name and Address [1]Civil Engineering Program Louisiana Tech University P.O. Box 10348 Ruston, LA 71272 [2]Louisiana State University Civil and Environmental Engineering 3502 CEBA Baton Rouge, LA 70803	10. Work Unit No. 99-3B 11. Contract or Grant No. State Project No. 736-99-0633
12. Sponsoring Agency Name and Address Louisiana Department of Transportation and Development Louisiana Transportation Research Center 4101 Gourrier Avenue Baton Rouge, LA 70808	13. Type of Report and Period Covered July 1998 – July 2003 14. Sponsoring Agency Code
15. Supplementary Notes	

16. Abstract

Experiment 2 at the Louisiana ALF site involved determining the engineering benefits of using powdered rubber (PRM) in hot mix asphalt mixes. Three full scale test sections were constructed and subjected to increasing loads from the ALF. Lane 2-1 included PRM in the wearing course, lane 2-2 included PRM in the base course, and lane 2-3 was the control section.

Distress and deflection measurements were performed every 25,000 applications of the ALF. Laboratory material characterizations of test lane materials were used in ABAQUS and FLEXPASS modeling studies to predict the behavior and performance of the test lanes. Comparisons of observed and predicted rutting were developed and discussed. Deflection measurements were used to develop a-values for the powdered rubber modified layers for use in pavement design. The recommended a-value for the PRM wearing course was 0.25; it was 0.45 for the PRM base.

17. Key Words powdered rubber, crumb rubber, accelerated loading, full-scale testing, ABAQUS, FLEXPASS, performance modeling, rutting, soil cement, inverted pavement section	**18. Distribution Statement** **Unrestricted. This document is available through the National Technical Information Service, Springfield, VA 21161.**

19. Security Classif. (of this report) None	**20. Security Classif. (of this page)**	21. No. of Pages 97	22. Price

Comparative Performance of Rubber Modified Hot Mix Asphalt Under ALF Loading

by

Freddy L. Roberts
T.L. James Professor, Louisiana Tech University
Louay N. Mohammad
Associate Professor, Louisiana State University
Hanlin Qin
Graduate Research Assistant, Louisiana Tech University
Baoshan Huang
Graduate Research Assistant, Louisiana State University

State Project No. 736-99-0633
LTRC Project No. 99-3B

Conducted for

Louisiana Department of Transportation and Development
Louisiana Transportation Research Center

August 2003

ABSTRACT

To determine the engineering benefits of using powdered rubber in hot mix asphalt (HMA) mixtures, three test lanes were constructed at the Louisiana Pavement Research Facility (PRF) in Port Allen, Louisiana. The objectives of this study were to compare the performance of powdered rubber modified (PRM) HMA with that of conventional HMA materials, to identify the optimal location in the pavement structure to use the PRM HMA, and to determine the structural coefficients for the PRM HMA used in wearing and base course layers. Lane 2-1 had a PRM HMA wearing course, Lane 2-2 had a PRM HMA Type 8 binder modified base layer, and Lane 2-3 was built from conventional materials. Conventional materials included Type 8 wearing course and binder course with a polymer modified binder (3 percent polymer), and a base course with AC 30 asphalt. All pavements were designed to have a 1.5 in. wearing course, 2.0 in. binder course, 3.5 in. base course, 8.5 in. crushed stone base and 10.0 insoil cement over the embankment soil at the site. Test lanes were constructed with conventional construction equipment and quality assurance tests were performed by Louisiana Department of Transportation and Development (LaDOTD) personnel.

Axle loads were applied to the pavement in increments of 25,000 applications by the Accelerated Loading Facility (ALF). A rotation scheme was used in an attempt to keep environmental conditions similar for all three lanes. After each rotation, condition surveys, deflection surveys, and transverse profiles were secured. The collected data was used to compare performance and to determine the relative strength coefficients of the PRM HMA layers.

Simulations of pavement behavior and performance were generated using two computer programs: ABAQUS and FLEXPASS. A 3-D dynamic simulation of pavement response was developed using ABAQUS based on laboratory fundamental engineering properties and actual ALF loads applied. Measured pavement responses from both the Dynaflect and Falling Weight Deflectometer (FWD) were compared to predicted responses using ABAQUS. The FLEXPASS model predicts performance using relationships between laboratory material properties and estimated pavement responses to predict the accumulated rutting, fatigue cracking, and roughness development for the test lanes.

Deflection responses of the test lanes during ALF testing were used to predict the structural coefficients (SN) for the PRM HMA wearing course and base course. Comparisons were made between SN values predicted from the Dynaflect and FWD and those resulting from back calculation of SN from the AASHTO flexible pavement design equation. These results were presented and discussed and values calculated from FWD results were recommended for use by LaDOTD in pavement design.

ACKNOWLEDGMENTS

The authors would like to acknowledge the assistance of the staff at the Pavement Research Facility for their work in collecting the field data that was essential for the completion of this project. We extend our thanks to Bill King, PRF manager; Keith Gillespie, electronics specialist; George Crosby, mechanical specialist; and the undergraduate students who worked during Experiment 2. We are also very fortunate to have worked with Masood Rasoulian, manager of pavement research at LTRC, who has been helpful and understanding as this project was extended several times because these pavements exhibited superior performance. We would also be remiss not to express our thanks to the graduate and undergraduate students who tested pavement materials in the laboratories at LTRC. We also want to thank the various LTRC technicians who were responsible for performing the Dynaflect and Falling Weight Deflectometer tests, which were crucial in determining the structural coefficients for the powdered rubber materials.

Finally, we want to express our gratitude for the support of the Louisiana Department of Transportation and Development for the funds to construct and test the lanes at the PRC. National interest in this research occurs because of the provisions of the 1991 ISTEA legislation. Even though the provisions of that legislation that mandated the use of discarded tire rubber in hot mix asphalt were dropped, the issue of disposal of waste tire rubber is still an unresolved national issue. This research clearly indicates that powdered rubber from discarded tires can be efficiently and economically used in highway construction.

IMPLEMENTATION STATEMENT

The Louisiana Department of Transportation and Development (LaDOTD) should begin to either add powdered rubber modifier to the AC-30 currently used in base courses or to replace the AC-30 with PAC-40 asphalt in those bases. This substitution improves the structural coefficient, a-value, of the base by 12.5 percent, increasing the a-value from the current value of 0.40 to 0.45. The addition of 10 percent powdered rubber to the AC-30 increased the cost of the binder by approximately 10 percent, which is about what the polymer costs to make the PAC-40 material currently used in the wearing and binder courses.

In addition, the superior performance of all three test lanes demonstrates again the efficiency of the inverted pavement section in which a stiff layer of soil cement is covered with a layer of stone that then has a combination of asphalt base, asphalt binder and asphalt wearing courses applied. In previous experiments conducted at the PRF, the superior performance of the inverted section was demonstrated. These sections are very strong and resistant to rutting and experience no reflection cracking from the soil cement layer. In fact, no cracking was observed in any of the test lanes in the current experiment.

TABLE OF CONTENTS

LIST OF TABLES

LIST OF FIGURES

INTRODUCTION

Problem Statement

Waste or scrap tires pose a substantial waste management challenge due to the large number of scrap tires generated annually throughout the nation. In order to reduce scrap tire inventories, applications and markets for scrap tire rubber have to be developed and enhanced. In 1991, the Intermodal Surface Transportation Efficiency Act (ISTEA) specified that any asphalt pavement project funded by federal agencies must contain a certain percentage of scrap tire rubber *[1]*, *[2]*. Although this mandate was dropped from the ISTEA legislation, it did encourage the research and application of hot mix asphalt (HMA) materials that include crumb rubber modifier (CRM) in pavement construction.

CRM has been used in asphalt pavement construction for over 40 years principally as local patch repair material, as interlayers, or in seal coat construction. Since 1960, shredded waste tires have been used in asphalt mixtures. It was not until the late 1980s that the use of recycled tire crumb rubber in open graded friction courses became popular. However, it was used very little in dense graded HMA at that time.

One of the principal unresolved issues regarding the use of recycled rubber in asphalt pavement is the actual field performance of the material. When material characterizations from laboratory testing have been used in computer models like VESYS, the models have generally predicted better performance for the CRM-HMA than has been observed in the field. Because of the need to evaluate the engineering benefits of using CRM, to determine the optimal position within the pavement structures for these materials, to dispose of tires in an economical fashion, and to determine the appropriate structural coefficient for use in pavement thickness design, a field study was necessary to evaluate the performance of HMA materials that include CRM. Full-scale testing using the Accelerated Loading Facility (ALF) provided the best alternative for a relatively quick assessment of the cost-effectiveness of CRM-HMA.

Background of Project

The two aspects concerning the use of CRM in HMA materials are the environmental and engineering benefits. Many state highway and private sector agencies have conducted

their own research on the applications of crumb rubber in HMA mixtures. The findings on environmental benefits are widely accepted. However, there is no agreement among state agencies on the engineering benefits of using CRM in HMA pavement. In order to define the circumstances in which the Louisiana Department of Transportation and Development (LaDOTD) can use rubber in HMA materials in the most cost-effective way, full-scale testing was conducted by the Louisiana Transportation Research Center (LTRC) to evaluate the performance of rubber modified HMA pavements under accelerated loads. Two rubber modified HMA mixtures were designed: (1) a Louisiana Type 8 wearing course and (2) a base course mixture. The rubber modifier material selected for use in these projects was powered rubber modifier (PRM). Three ALF test lanes were constructed at the Louisiana Pavement Research Facility (PRF): one with conventional mixtures, one with a PRM-HMA Type 8 wearing course and one with a PRM-HMA base course. The conventional materials used in wearing and binder courses in Louisiana consist of a HMA with a binder to which three percent polymer has been added. Measured performance data will be used to evaluate the cost effectiveness of materials used in the test lanes. Additionally, performance predictions will be generated using numerical simulations of the test lanes, and the predicted performance will be compared with the observed field performance.

Review of Relevant Literature

Asphalt Rubber in Pavements

Generally, tire rubber that is ground to crumb form prior to use is designated as Crumb Rubber Modifier (CRM). Asphalt Rubber (AR) is asphalt cement to which 17 – 25 percent scrap rubber has been added and reacted at elevated temperature for a period of time. When CRM is added to asphalt cement, the rubber particles will generally swell in the asphalt, increasing viscosity of the blend.

Tire rubber has been used as an additive to asphalt cement in various applications in highways for over 40 years although the use of natural rubber in asphalt cement dates from the 1840s *[3]*. The concept of adding ground tire rubber to asphalt cement was developed in the 1950s *[4]*. Flintseal Corporation and U.S. Rubber Reclaiming reacted crumb rubber and asphalt cement in the laboratory in the early 1960s *[5]*. Charles H. McDonald, a consulting engineer from Phoenix, Arizona was one of the early users of the asphalt-rubber systems in the United States. His laboratory work, which was initiated in 1963, resulted in the placement of patching materials at Sky Harbor Airport in Phoenix in the mid 1960s *[5]*.

In 1975, Arizona Refining Company (ARCO) began experimental work with asphalt-rubber binder systems. ARCO's first experimental section was placed in 1975. The result of the experimental work conducted by McDonald and ARCO led to the use of rubber modified asphalt as a potential binder system across the United States and Canada. The Federal Aviation Administration (FAA) sponsored research involving laboratory testing and developing a mix design procedure for asphalt-rubber concrete for civil airport pavements from 1983-86 *[6]*. In 1989, Florida DOT began constructing demonstration projects of asphalt pavement with crumb rubber prepared using a wet process and they have reported satisfactory pavement performance *[7]*. California first began using asphalt rubber to improve the durability of HMA. With additional experience, California developed design guidelines in 1992 that allowed a reduction in overlay thickness for a gap-graded HMA with asphalt rubber for specific types of applications. Two wet processes (McDonald and Rouse) for reacting the rubber were used in Virginia in 1996. Results indicated that the inclusion of asphalt rubber in HMA pavements increased construction cost by 50 to 100 percent when compared to the cost of conventional mixes *[8]*. Troy et al conducted research of rubber modified asphalt mixtures in Nevada, *[9]*. In the Nevada study, the rubber modified binder was evaluated using the Superpave binder testing protocols while the mix design was developed using the Hveem procedure *[9]*.

Laboratory results from previous research indicate that asphalt rubber materials experience reduced thermal and reflective cracking, reduced rutting, and slower aging when compared to conventional mixes *[7]*. However, Page determined that a field evaluation was needed to determine whether these laboratory benefits actually occur in normal service *[7]*.

There are currently two methods for incorporating rubber in HMA: a wet process and a dry process. In the dry process, a coarse graded rubber is used as an aggregate with no opportunity for the asphalt and rubber to react before mixing with aggregate. In the wet process, the rubber is blended with asphalt cement prior to the mixing operation *[3]*. In the wet process, the rubber fully reacts with the asphalt binder and changes the binder properties. Common wet process methods include the McDonald, Ecoflex, and Wet Rouse continuous blending method *[3]*.

Previous ALF Testing

ALF is a full-scale transportable pavement test device that simulates the effect of traffic loading on full-scale pavements by applying controlled wheel loading in a repetitive

manner *[10]*. The machine was first designed and manufactured for AUSTROADS by the Road Transport Authority (RTA) in New South Wales, Australia *[11]*. In 1984, the FHWA purchased the U.S. manufacturing rights from the RTA, and the first ALF machine in the U.S. was assembled and located at the Turner-Fairbanks Highway Research Center (TFHRC). The second one was purchased by LTRC and delivered to the Pavement Research Facility outside Port Allen, Louisiana in April 1993. ALF can provide many benefits to highway agencies. Principal among these is the ability to observe the behavior and the damage patterns that develop under traffic loads in a short period of time. Such testing avoids the need for full-scale pavement tests like the AASTHO Road Test. Another benefit derived from ALF research is the ability to compare performance of a new material with a conventional material. Before being extensively used, the performance of a new material can be evaluated and its cost effectiveness assessed over a short period of time versus years required for in-service pavements.

The FHWA ALF has been in nearly continuous operation since its delivery in 1986. Bonaquist et al. used the ALF to evaluate the effects of tire pressure on flexible pavement response and performance *[12]*. Sebaaly et al. used data from previous ALF research to evaluate the relationships between surface cracking and the structural capacity of both thin and thick pavements *[13]*.

Loading of the first LTRC ALF experiment began in January 1994. The objective of the first experiment was to compare the performance of the mixed in-place soil cement stabilized base construction with several promising alternative base materials. Nine pavement test sections were constructed. The testing was divided into three phases of three test sections. Phase 1 testing compared crushed stone base alternatives to soil cement. Phase 2 was designed to compare the performance of plant-mixed soil cement design and construction with that of normal mixed in-place soil cement construction. Phase 3 included a comparison of mixed in-place soil cement design and construction procedures with that of a plant mixed soil cement process using a reduced cement content *[14]*. Results from this first ALF experiment can be found in *[15]*, *[16]*, *[17]*.

The comparative performance of rubberized asphalt hot mix is the second ALF experiment in Louisiana. ALF loading for this experiment began in March 1999 and ended in December 2000. A detailed description of this experiment is included in this report.

Numerical Simulation of Pavement Behavior

Numerical simulations of flexible pavements are important for understanding and extending the results of laboratory and field studies *[18]*. Structural analysis of pavement is usually performed to calculate responses such as stresses, strains, and deflections in a layered pavement structure. The methodologies available to determine the flexible pavement responses can be categorized as multi-layered elastic, multi-layered viscoelastic, and finite element methods *[19]*.

The multi-layered elastic method models a pavement as a series of layers, each of which is assumed to be a horizontally continuous, isotropic, homogenous, and elastic medium. Each layer has definite thickness except for the bottom layer, which is assumed to be semi-infinite in depth. The surface loading is represented by vertical contact pressure uniformly distributed around a circular area. The Poisson's ratio and the elastic modulus of each layer are the material parameters that control their behavior. A number of computer programs such as BISAR, CHEV, and ELSYM5 were designed to calculate stress and strain distributions in pavement systems using this method.

Layered elastic analytical solutions provide one approach for pavement structural analysis. However, they oversimplify the asphalt material behavior by assuming linear elasticity. Multi-layered viscoelastic methods are similar to the multi-layered elastic method, except that the pavement material properties vary with loading time and temperature. Software such as VESYS and MICH-PAVE utilize viscoelastic models for the HMA and linear elastic or nonlinear elastic models for the base course and subgrade materials *[19]*,*[20]*.

Finite element method (FEM) is a technique in which the body to be analyzed is divided into a set of finite elements connected at their nodal points. The continuous variation of stresses and strains in the body is represented by an assumed linear or quadratic displacement function over each finite element. For a given element geometry and constitutive equation describing material behavior, the element stiffness matrix can be established using the principle of virtual work. The global structural stiffness can then be formulated by integrating the individual element stiffness matrices. The result is a set of simultaneous equations that reflect the unknown displacement of nodes and the loading force. Solving these equations using Gaussian elimination produces all nodal displacements. With the calculated nodal displacements, strains and stresses within each element can be calculated.

FEM is most useful in calculating the response of pavement structure when pavement material behavior is nonlinear elastic, viscoelastic, or elasto-plastic. ILLPAVE and FLEXPASS are two software programs which use finite element methods to predict pavement structural behavior. Lytton and Tseng calibrated the rutting and fatigue models by comparing the actual measurements of 12 AASTHO road test sections to the predicted distress from FLEXPASS *[20]*. Hoyt et al., compared predicted performance of asphalt-rubber concrete to that of hot mix asphalt in airfield runways by using FLEXPASS *[6]*.

ABAQUS is another general-purpose finite-element program that can solve problems ranging from relatively simple linear analyses to the most challenging nonlinear simulations. Zaghloul applied three dimensional finite element analyses to simulate dynamic traffic loads using ABAQUS *[21]*. Wathugala and Huang et al. analyzed the behavior of geosynthetic-reinforced flexible pavements in a finite element model by using ABAQUS *[22]*.

In this analytic procedure, FLEXPASS is used for pavement performance prediction. The advantage of using FLEXPASS is that it is a 2-D finite element model of a layered flexible system and it is compatible with 2-D finite element models used in ABAQUS for response analysis. It is the only finite element program that has the capabilities of including multiple tire – multiple axle assemblies, predicting distress, representing actual tire contact pressure distributions, and considering seasonal variations of material properties.

OBJECTIVES

The objectives of this study were:

- To evaluate the overall performance of hot mix asphalt mixtures containing powdered rubber modifier (PRM) as compared to similar mixes with conventional HMA under ALF loading.

- To identify the optimal location in the pavement structure that the LaDOTD can use powdered rubber materials in the most cost-efficient manner.

- To evaluate the structural analysis responses of hot mix asphalt mixtures containing PRM as compared with similar mixes with conventional HMA under ALF loading.

- To determine appropriate structural coefficients, a-values, for use of these materials in the structural design of flexible pavements using the AASHTO design procedure.

SCOPE

To achieve these objectives, three test lanes were constructed at the Louisiana ALF site using conventional and rubberized HMA. ALF loads were applied until failure occurred using the selected failure criteria.

The second part of this study involved conducting numerical simulation of ALF test lanes using two finite element programs: FLEXPASS and ABAQUS. The finite element computer software called FLEXPASS was used for performance prediction. The input parameters for FLEXPASS were based on the results from laboratory tests performed on pavement materials from the ALF site and field information. The predicted performance includes rutting, fatigue cracking, slope variance and present serviceability index (PSI). A three-dimensional dynamic finite element analysis was used in this study to calculate the primary responses, stress and strain, of the pavement to the applied loads. The input parameters for ABAQUS were developed from laboratory testing and the predicted pavement responses were compared to experimental measurements made on ALF test sections.

The third part of this study involved comparing the field performance of the three test lanes to predicted performance of the same three lanes. The specific comparison of performance was made for HMA and powdered rubber materials in the surface and base position for these three lanes subjected to ALF loading.

The fourth part of this study involved using both data collected during testing of the test lanes and performance predictions to calculate a-values for the layers including powdered rubber materials.

The performance was evaluated using the number of applied loads, observed distresses at specified loading intervals, pavement response to non-destructive testing, and comparisons between predicted and observed performance measures.

METHODOLOGY

Description of Research Methodology

The project consisted of construction, field loading and testing, laboratory characterization, and numerical simulation of the three test lanes at the Louisiana Pavement Research Facility under accelerated loading. The experiments were designed so that paired comparisons could be made between the powdered rubber modified HMA in the surface and the base with conventional HMA in the surface and the base. For specific information regarding section design, materials, construction, evaluation plan and instrumentation for the test lanes, refer to King and Abadie *[10]*.

Design and Construction of ALF Experiment

Design of Pavement Cross Section. The first lane was designed to have the powdered rubber modified HMA (PRM-HMA) in the surface layer; the second lane was designed to have the PRM-HMA in the base layer; and the third lane was designed as the control lane consisting of conventional mix throughout the layer. Table 1 shows the planned cross sections of the three test lanes.

Table 1
Structure of test lanes

Lane 2-1	Lane 2-2	Lane 2-3[1]
1.5”(38 mm) Type 8F Wearing Course (PRM wet Rouse binder)	1.5” (38 mm) Type 8F Wearing Course (PAC 40 binder)	1.5” (38 mm) Type 8F Wearing Course (PAC 40 binder)
2.0” (51 mm) Type 8 Binder Course (PAC 40 binder)	2.0” (51 mm) Type 8 Binder Course (PAC 40 binder)	2.0” (51 mm) Type 8 Binder Course (PAC 40 binder)
3.5” (89 mm) Base Course (AC 30 binder)	3.5” (89 mm) Base Course (PRM wet Rouse binder)	3.5” (89 mm) Base Course (AC 30 binder)
8.5” (216 mm) Crushed Stone	8.5” (216 mm) Crushed Stone	8.5” (216 mm) Crushed Stone
10.0” (254 mm) Soil Cement	10.0” (254 mm) Soil Cement	10.0” (254 mm) Soil Cement
38.0” (965 mm) Select Soil/Embankment	38.0” (965 mm) Select Soil/Embankment	38.0” (965 mm) Select Soil/Embankment

[1]Lane 2-3 is the control lane with conventional materials where the wearing and binder courses include a polymer modified asphalt**.**

Selection of Materials and Mix Design

Asphalt cement. LaDOTD specifies that PAC-40 asphalt cement, which consists of an asphalt modified with an elastomer, be used in binder and wearing course mixtures. An AC-30 was used for the conventional base course mix. The AC 30 asphalt cement was combined in a "wet process" with 10 percent of a No. 80 mesh powdered rubber at 400°F (205°C) for approximately an hour to produce the modified binder. The powdered rubber was chosen over crumb rubber based on performance of field projects previously

Table 2
Asphalt binder test summary *[10]*

Description	AC-30	AC-30w/ PRM	PAC-40	AASHTO Specs.	AASHTO Method
Original Binder					
Rotational Viscosity; Brookfield, Pa-s, 275°F (135°C)	0.463	3.10	1.05	3.0	TP48
Force Ductility, ratio of final/max load	Fail	Fail	Pass	0.3	
Dynamic Shear Rheometer, DSR, G*sinδ, kPa, @10rad/s					
147°F (64° C)	1.7274	3.0659		1.0min	TP5
153°F (67 °C)	1.2146		2.7328	1.0min	TP5
158°F (70°C)	0.8405	2.3991	1.8974	1.0min	TP5
169°F (76°C)		0.8914	1.0156	1.0min	TP5
RTFO (TFO for PRM-HMA)					
% Loss		0.1	0.187	1.0max	TP240
147°F (64°C)		6.6001		2.2min	TP5
153°F (67°C)	3.488	4.2759		2.2min	TP5
158°F (70°C)	2.2942	3.218	3.2058	2.2min	TP5
169°F (76°C)		1.7412	1.8564	2.2min	TP5
PAV					
DSR, G*xsinδ, kPa, @10rad/s @ 77°F (25°C)	3628.3	2122.6	3175.1	5000max	TP5

constructed in Louisiana. Daly et al. reported that crumb rubber can be blended at rates higher than 10 percent, but separation and possible incompatibility is more likely to occur with some crude suppliers in Louisiana when more than 10 percent is used *[23]*. The

AC-30 met the superpave PG 64-22 specification; the AC 30 and PRM blend met a PG 70-22 specification, as did the PAC-40. Table 2 shows the properties of the asphalt binders used in this study. It should be noted that the PAC-40 asphalt and the AC-30 with PRM exhibit very similar shear characteristics when tested with the Dynamic Shear Rheometer (DSR) for both the virgin and aged materials. Notice especially the similarities in the test values at 158^{o}F (70^{o}C) and 169^{o}F (76^{o}C) for both virgin and aged materials. This similarity in test values of the PAC-40 and AC-30 with PRM indicates that these materials should demonstrate similar performance in the field.

Aggregates. The No.5, No. 67 and No. 78 coarse aggregates and No. 11 screenings were all siliceous limestone supplied by Vulcan Materials Company, from the Reed quarry in Gilbertsville, Kentucky. Coarse siliceous sand was supplied by Quick Sand and Gravel from Watson, Louisiana. Table 3 lists the properties of the aggregates.

Table 3
Aggregate properties *[10]*

Aggregate		FAA Method	Sand Equivalent	Flat & Elong % 5:1	CAA +two faces	Friction Rating	LA Abrasion
Source	Type						
Vulcan Reed	No.5			3	100	II	20.1%
Vulcan Reed	No.67			3	100	II	20.1%
Vulcan Reed	No.78			2	100	II	20.1%
Vulcan Reed	No.11	47	44				
Quick Sand and Gravel	coarse sand	43	61				
Mamonth Dr	RAP				100		

Mix Design. The Marshall mix design procedure was used to design all mixtures. The nominal maximum aggregate size of the wearing course mixture was 0.75 in. (19 mm), while that of the binder and the base courses was 1.0-in. (25mm). The same aggregate structure was used for both the binder course and base course mixtures. The contractor took advantage of a specification-permitted opportunity to substitute a higher level of mix type, in this case a binder course mix replaced of the Type 5A base. In effect, he used an

approved binder course job mix formula for both the 2.0 in. (51-mm) binder course (with an PAC 40 asphalt) and the 3.5 in. (89-mm) base course (with an AC 30 asphalt). The binder and base course mixtures contained 20 percent RAP. All the gradations were on the "fine side" of the maximum density line. Table 4 includes the standard Marshall properties of the mixes.

Table 4
Marshall mix properties of the mixes *[10]*

TEST DESCRIPTION	ASPHALT MIX DESCRIPTION				
	Type 8 Wearing (with PAC40)	Type 8 Wearing (with PRM)	Type 8 Binder (with PAC 40)	Base (with AC30)	Base (with PRM)
Theoretical	2.531	2.531	2.533	2.533	2.531
G_{mm}	2.493	2.509	2.509	2.507	2.509
% AC By Weight	4.0	4.0	3.5	3.5	3.5
% AC By Volume	9.4	9.4	8.3	8.3	8.2
% Voids Total Mix	3.9	4.4	4.1	4.0	4.6
%VFA	70.8	68.2	66.6	67.5	64.0
%VMA	13.3	13.8	12.4	12.3	12.8
Unit Wt. Total Mix	151.8	151.0	151.5	151.8	150.6
Stability-lbs	2430	1904	2810	2711	2455
Flow	9	19	10	10	7

Mixture Characterization Tests

In the laboratory, each mixture was characterized using fundamental engineering property tests. These tests included the indirect tensile strength (ITS), indirect tensile resilient modulus (M_R), indirect tensile creep (IT-CRP), axial creep (AX-CRP), Superpave simple shear frequency sweep at constant height (FSCH) and repetitive shear at constant height (RSCH) tests. Asphalt mixture specimens for the tests listed above were prepared using the U.S. Army Corps of Engineers Gyratory Testing Machine (GTM) and the Superpave Gyratory Compactor (SGC) from plant produced materials. There were two specimen sizes: 4.0 in. (101 mm) in diameter by approximately 2.5 in. (63 mm) in height made from GTM and 6.0 in. (150 mm) in diameter by approximately 4.7 in. (120-mm) in height made from the SGC. The 6.0 in. (150-mm) diameter specimens made by the SGC were cut into 2.0 in. (50 mm) thick specimens for the

Superpave shear tester (SST) protocols. At the target air void levels (7 percent for the SST tests and 4 percent for the other tests), specimens were statistically grouped in triplicate sets to have similar mean air void levels. Indirect tensile strength (ITS) tests at 77°F (25°C), indirect tensile resilient modulus (M_R) tests at three temperatures 40, 77 and 104°F (4, 25, 40°C), and indirect tensile (IT-CRP) and axial creep (AX-CRP) tests at 104°F (40°C) were conducted. In addition, the Superpave frequency sweep at constant height (FSCH) test was conducted to determine viscoelastic properties of the asphalt mixtures that include dynamic shear modulus (G^*) and shear phase angle (δ) at 140°F (60°C). Repeated shear test at constant height and repeated shear test at constant stress ratio were used to evaluate permanent deformation behavior of the asphalt mixture. Table 5 presents the tests performed for each mixture.

Table 5
Test factorial for mixture characterization

Tests	Sample Size D x H, inch (mm)	Test Temperature °F(°C)	Mixtures			
			T8 WC (with PAC 40)	T8 WC (with PRM)	Base (with AC 30)	Base (with PRM)
ITS	4.0x2.5 (101 x 63)	77 (25)	3	3	3	3
M_R	4.0x2.5 (101 x 63)	40, 77, 104 (4, 25, 40)	3,3,3	3,3,3	3,3,3	3,3,3
IT-CRP	4.0x2.5 (101 x 63)	104 (40)	3	3	3	3
AX-CRP	4.0x2.5 (101 x 63)	104 (40)	3	3	3	3
FSCH	6.0x2.0 (150 x 50)	140 (60)	3	3	3	*
RSCH	6.0x2.0 (150 x 50)	140 (60)	3	3	3	*

*Specimens were not available

Indirect Tensile Strength (ITS) Test

The indirect tensile strength (ITS) and strain test was used to determine the tensile strength and the evolution of the strain of the mixtures. This test was conducted at 77°F (25°C) according to AASHTO T245. Each test specimen was loaded to failure at a 2 in./min (50.8 mm/min) deformation rate. The load and deformations were continuously recorded and indirect tensile strength and strain were computed as follows:

$$S_T = \frac{2 \cdot P_{ult}}{p \cdot t \cdot D} \quad (1)$$

$$e_T = 0.0205 H_T \quad (2)$$

where

S_T – Tensile strength, kPa
P_{ult} – Peak load, N
t – Thickness of the specimen, mm
D – Diameter of the specimen, mm
e_T – Horizontal tensile strain at failure, mm/mm, and
H_T – Horizontal deformation at peak load, mm.

The toughness index (TI) is a parameter that describes the toughening characteristics in the post-peak region. It is computed from the indirect tensile test results. Figure 1 presents a typical normalized indirect tensile stress and strain curve. A dimensionless indirect tensile toughness index, TI, is defined as follows:

$$TI = \frac{A_e - A_p}{e - e_p} \quad (3)$$

where

TI – Toughness index,
A_e – Area under the normalized stress-strain curve up to strain e,
A_p – Area under the normalized stress-strain curve up to strain e_p
e – Strain at the point of interest, and
e_p – Strain corresponding to the peak stress.

The toughness index compares the performance of a specimen with that of an elastic perfectly plastic reference material, for which the TI remains a constant of 1. For an ideal brittle material with no post-peak load carrying capacity, the value of TI equals zero. A similar analysis was reported by Soban et al. where the values of indirect tensile toughness index were calculated up to tensile strain of three percent *[24]*.

Indirect Tensile Resilient Modulus (M_R) test

At test temperatures of 40, 77, and 104°F (4, 25, and 40°C), this test was conducted according to the modified ASTM D 4123 *[25]*. It is a repeated load indirect tension test for determining the resilient modulus of the asphalt mixtures. The recoverable vertical deformation *V and horizontal deformation *H were used to calculate the indirect tensile

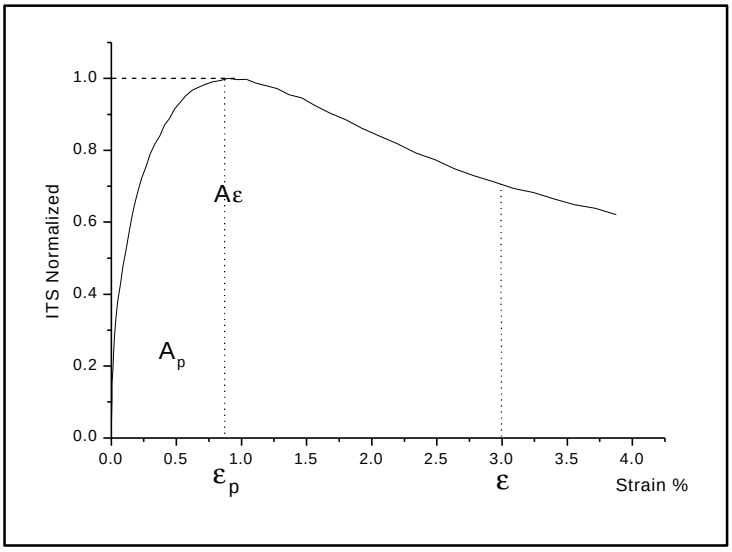

Figure 1
A typical normalized ITS curve for toughness index calculation

resilient modulus, M_R and Poisson's ratio, as shown in Equations 4 and 5.

$$M_R = \frac{P \cdot (m + 0.27)}{t \cdot dH} \quad (4)$$

$$m = 3.59 \cdot \frac{dH}{dV} - 0.27 \quad (5)$$

where

M_R – Resilient Modulus, MPa,
P – applied vertical load, N,
t – sample thickness, mm,
m – Poisson's ratio,
dH – horizontal deformation, mm, and,
dV – recoverable vertical deformation, mm.

Indirect Tensile Creep (IT-CRP) Test

At 104°F (40°C) a compressive load of 250 lbf (1.110 kN) was applied to the specimen using the stress-controlled mode of the MTS test system. The load was applied for 60 minutes or until the specimen failed *[25]*. The deformations acquired during this time were used to compute the creep modulus as follows:

$$S(T) = \frac{3.59 \cdot P}{t \cdot dV(T)} \tag{6}$$

where, $S(T)$ – creep modulus at time T, MPa,
P – applied vertical load, N,
t – sample thickness, mm, and
$dV(T)$ – vertical deformation at time T, mm.

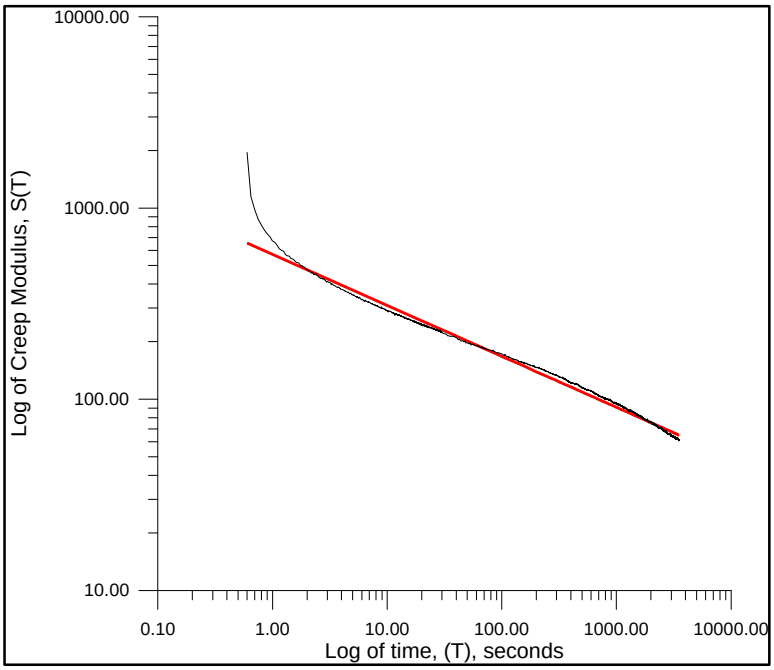

Figure 2
Typical curve of IT creep modulus

Figure 2 shows a typical creep modulus versus time graph on a log-log scale for the indirect tensile creep data. The graph slope was computed from this graph and used in the analysis.

Axial Creep (AX-CRP) Test

This test was conducted in accordance with the Test Method Tex-231-F *[26]*. A static load of 125 lbf (0.555 kN) was applied for the duration of one hour along the centric longitudinal axis of the specimen. The axial deformation of the specimen is continuously measured and subsequently used to calculate creep properties such as stiffness, slope, and permanent strain. These data are used to evaluate the permanent deformation characteristics of asphalt mixtures. Figure 3 presents a typical creep curve from the axial creep test.

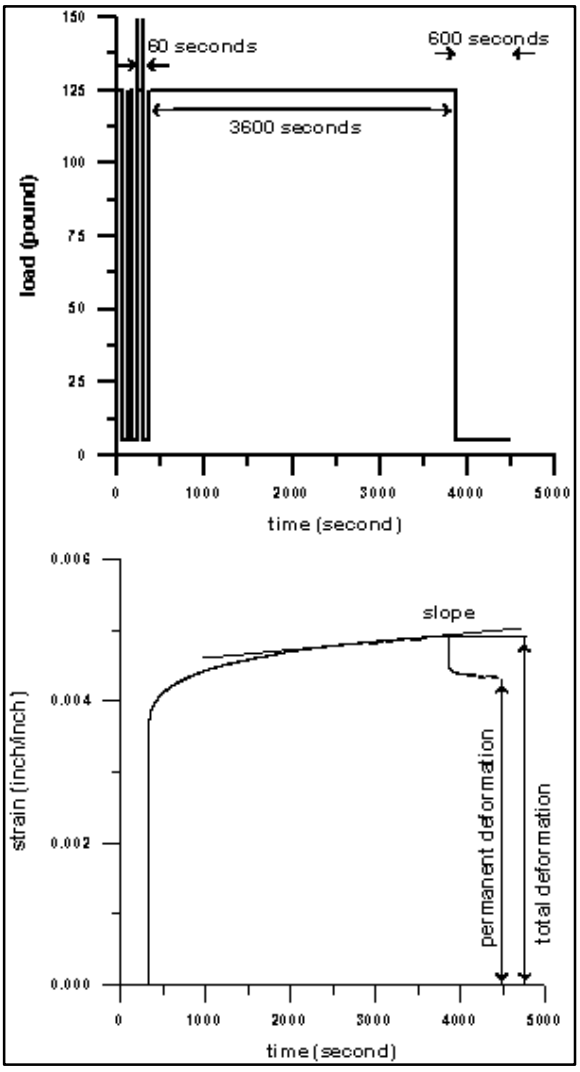

Figure 3
A typical axial creep curve

Frequency Sweep at Constant Height (FSCH) Test

This test, conducted in the shear mode (Figure 4), is a strain-controlled test in which a specific amount of deformation is induced in the specimen at 140^{o}F (60^{o}C). Stress generated in the specimen is measured but not controlled. The sinusoidal shear strain with peak amplitude of approximately 0.05 ③inch/inch (i.e. 50 micro strain) is applied at frequencies of 10, 5, 2, 1, 0.5, 0.2, 0.1, 0.05, 0.02 and 0.01 Hz. This strain level was selected during the SHRP Research Program to ensure that the viscoelastic response of the asphalt mixture is within the linear range, meaning that the ratio of stress to strain is a function of loading time (or frequency) and not of the stress magnitude. An axial stress is applied to maintain constant height. Frequency is directly related to traffic speed. For example, a frequency of 1 Hz corresponds to a traffic speed of 39 miles/hr (63 km/hr) *[27]*. Hence, a frequency sweep test can be used to evaluate the behavior of an asphalt mixture at different traffic speeds. Figures 5 and 6 present typical load and response curves of FSCH test.

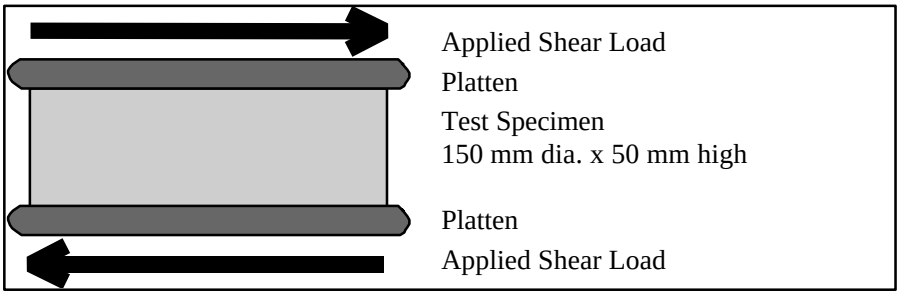

Figure 4
Specimen configuration of FSCH test

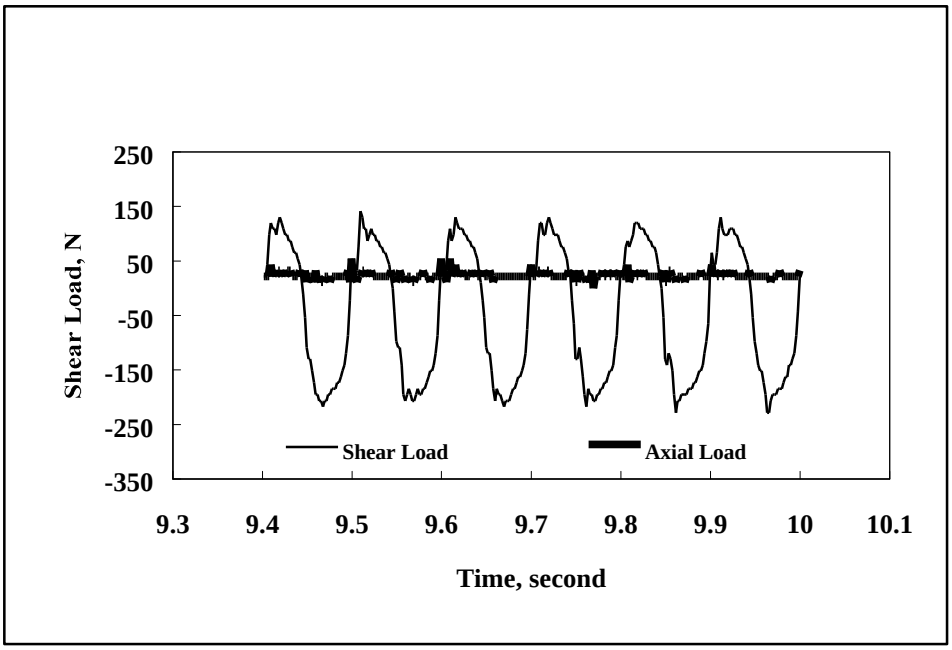

Figure 5
Loads during frequency sweep at constant height test

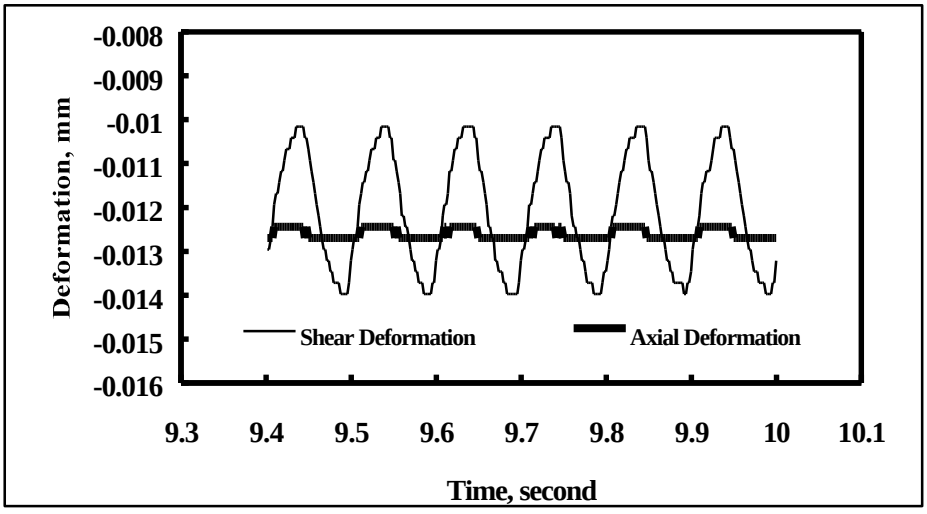

Figure 6
Deformations during frequency sweep at constant height test

Repetitive Shear at Constant Height (RSCH) Test

This is a stress-controlled test. A repetitive shear load (haversine) is applied to the specimen to generate a shear deformation. The shear load is applied with a maximum shear stress of 10 psi (68 kPa) for a loading time

of 0.1 seconds and a rest period of 0.6 seconds. Repetitive loading is applied for a total of 5,000 repetitions or until 5 percent shear strain occurs. An axial stress is applied to maintain constant height.

In development of the repeated shear test at constant height two mechanisms that provide resistance to permanent deformation in an asphalt mixture were hypothesized *[28]:*

1. Asphalt binder stiffness. Stiffer binders help in resisting permanent deformation as the magnitude of the shear strains is reduced under each load application. The rate of accumulation of permanent deformation is strongly related to the magnitude of the shear strains. Therefore, a stiffer asphalt will improve rutting resistance as it minimizes shear strains in the aggregate skeleton.

2. Aggregate structure stability. The axial stresses act as a confining pressure and tend to stabilize the mixture. A well-compacted mixture with a good granular aggregate will develop high axial forces at very small shear strain levels. Poorly compacted mixtures can also generate similar levels of axial stresses, but they will experience much higher shear strain.

In the constant height simple shear test these two mechanisms are free to fully develop their relative contribution to the resistance of permanent deformation as they are not constrained by imposed axial or confining stresses. The development of the repeated shear test at constant height was detailed elsewhere *[28]*.

Numerical Simulation and Analysis of ALF Test Lanes

Numerical Simulation Using ABACUS

To support the results from the ALF tests, a 3-D dynamic finite element analysis was performed on each test lane. White and his co-workers successfully used the 3-D dynamic finite element method to analyze the dynamic responses and the predicted permanent deformation of pavement under traffic loads *[18]*,*[21]*,*[29]*. In the current study, only primary responses (stress, strain) were utilized from the finite element analysis.

1. Geometric Models. Figure 7 illustrates the 3-D Finite Element (FE)mesh established for numerical simulation in this study. Twenty node-reduced integration brick elements were used to form the FE mesh. Due to symmetry, only half of the

pavement lane was modeled. Results from a sensitivity analysis indicated that a mesh of 6760 (52x13x10) elements would provide reasonable continuity for the pavement stresses and strains produced by the ALF loads.

2. Material Models. Elastoplastic (Drucker-Prager) models were used to describe the paving materials in the numerical simulation. Table 6 presents the material parameters used for numerical analysis in this study. Rate dependency was considered for the asphalt concrete material. In the commercial finite element software, ABAQUS*[30]*, the rate dependency in plastic material is expressed as:

$$f(s) = \bar{s}(\bar{e}^{pl}, \dot{\bar{e}}^{pl}, q, f^{a}) \tag{7}$$

$$\bar{s} = \left[1 + \left(\frac{\dot{\bar{e}}^{pl}}{D}\right)^{\frac{1}{n}}\right] \cdot s^{0} \tag{8}$$

Where s is the equivalent yield stress; e^{pl} is the equivalent plastic strain; e^{pl} is the equivalent plastic strain rate; q is the temperature; f^{a} is a function of a predefined field variable where a = 1, 2, …; and D and n are material parameters that determine the overstress ratio R, defined as:

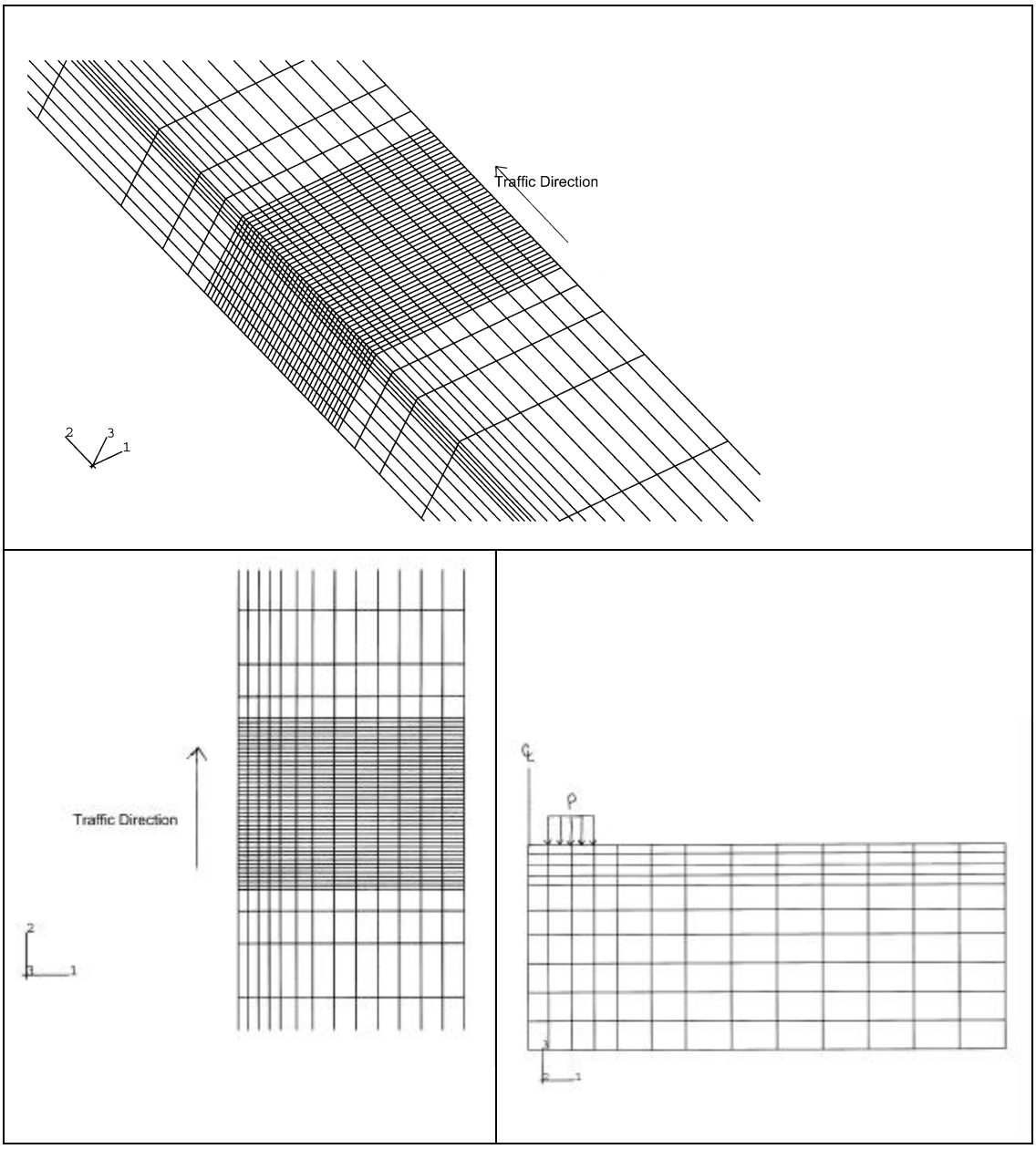

Figure 7
3-D finite element mesh

$$R = 1 + \left(\frac{\dot{e}^{pl}}{D} \right)^{\frac{1}{n}} \tag{9}$$

The static equivalent yield stress F^o includes plastic strain hardening and the overstress ratio represents the rate dependency. Figure 8 presents the dynamic yield surfaces of the asphalt mixture when using the Drucker Prager yield criteria.

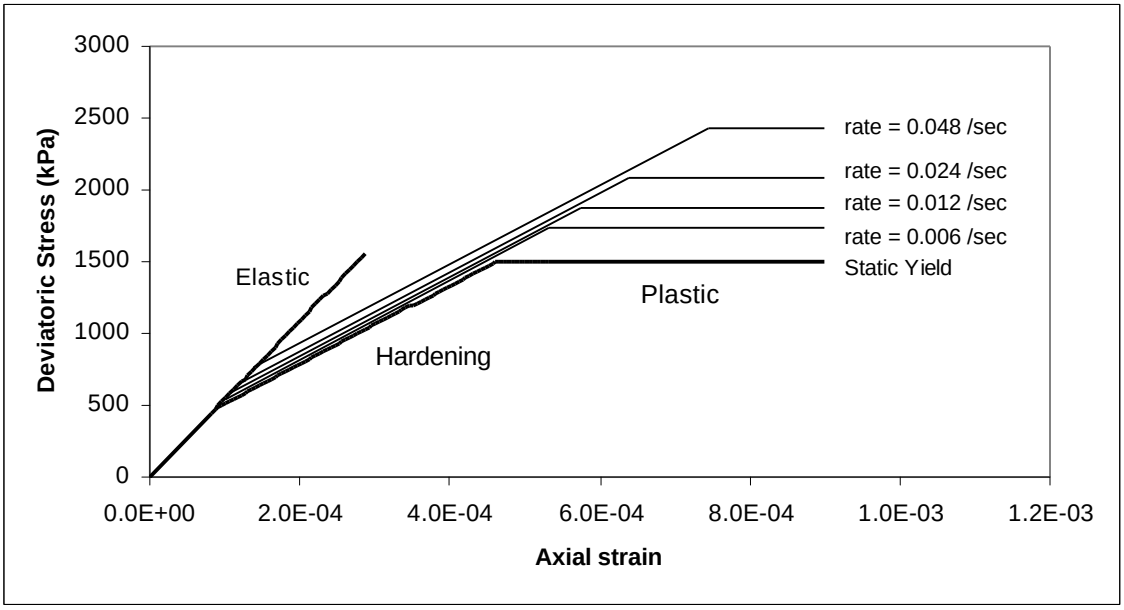

Figure 8
Dynamic yield functions of hot mix asphalt materials

Numerical Simulation Using FLEXPASS

In this study, FLEXPASS is used for pavement performance prediction. FLEXPASS has the ability to include seasonal variations of material properties.

Overview of FLEXPASS. Developed by Lytton and Tseng of the Texas Transportation Institute, FLEXPASS is a finite element program with the ability to accommodate multiple wheel loads and at the same time employ stress dependent material characterization models *[31]*. It is an extension of the widely used ILLIPAVE, which was originally developed by Wilson and Duncan, and further modified by the Department of Civil Engineering, University of Illinois, Construction Engineering Laboratory and Facilities Group in 1982 *[32], [33]*.

Table 6
Material parameters in finite element analysis

Material		HMA Layer	HMA Layer	HMA Layer	Crushed Limestone	Compacted Soil	Subgrade Soil
Lane No.		1	2	3	1,2 and 3	1,2 and 3	1,2 and 3
Thickness, inch (mm)		7.0 (176.8)	7.0 (176.8)	7.0 (176.8)	8.5 (215.9)	10.0 (254.0)	>10.0 (254.0)
Material Model		Visco Plastic	Visco Plastic	Visco Plastic	Drucker Prager	Drucker Prager	Drucker Prager
Elastic Modulus, E , ksi (kPa)		634 (4.38x $10^{6)}$	788 (5.44x 10^{6})	582 (4.02x 10^{6})	72.5 ($5.0x10^{5}$)	37.7 ($2.6x10^{5}$)	21.7 ($1.5x10^{5}$)
Poisson's Ratio, ν		0.35	0.35	0.35	0.35	0.30	0.45
Drucker Prager	K,kPa (psi)	68 (470)	68 (470)	58 (400)	2.17 (15)	11.6 (80)	7.2 (50)
	T,^{o}F (^{o}C)	104 (40)	104 (40)	104 (40)	122 (50)	86 (30)	68 (20)
Visco-plastic	D	0.1	0.1	1.0			
	n	1.5	1.5	1.5			

Lytton and Tseng took the finite element program, which could be used to predict flexible pavement responses, and added the capability to predict pavement performance in terms of rutting, fatigue cracking, slope variance and PSI loss *[31]*. A simplified flow diagram of FLEXPASS is shown in Figure 9.

This program was chosen because it offers the following capabilities:

- The finite element method permits pavement layers to be described using non-linear stress-strain relationships.

- An interface slip element is included to allow modeling of slip between adjacent pavement layers.

- The pavement material properties can be varied seasonally.

- The loading configurations can vary from single or dual tires on single or tandem axles.

The prediction algorithms for fatigue cracking, rutting, and serviceability loss are included to provide outputs which are used in the field to assess performance and have been calibrated using actual field data from the AASHTO Road Test.

Description of FLEXPASS Finite Element Model. The development of a numerical simulation of flexible pavements involves many idealizations of the problem, including geometry, loads, material property (constitutive) models, and selection of the numerical simulation technique. In this project, the pavement structure will be modeled using a 2-D half space of a finite solid of revolution as shown in Figure 10. The half-section structure to be analyzed is divided into a set of quadrilateral finite elements, which are then divided into four triangles by the program to produce a set of elements. The tire contact pressures are assumed to have a vertical uniform distribution over a circular contact area. Material properties such as density, Poisson's ratio, earth-pressure coefficient at rest, and resilient modulus are required as inputs in the program. Two significant material response capabilities, both linear and nonlinear stress-strain relations, can be utilized. The failure criteria for granular and fine-grained soils are considered.

Four alternative models are available for describing the resilient modulus of the pavement materials *[34]:*

1. Linear Resilient Modulus. This model assumes that the material has a linear resilient modulus relationship with temperature. Hot mix asphalt and PRM HMA are characterized using this model.

2. Bulk Stress Dependent Modulus. This model describes the resilient modulus of granular material as a function of bulk stress. The equation is:

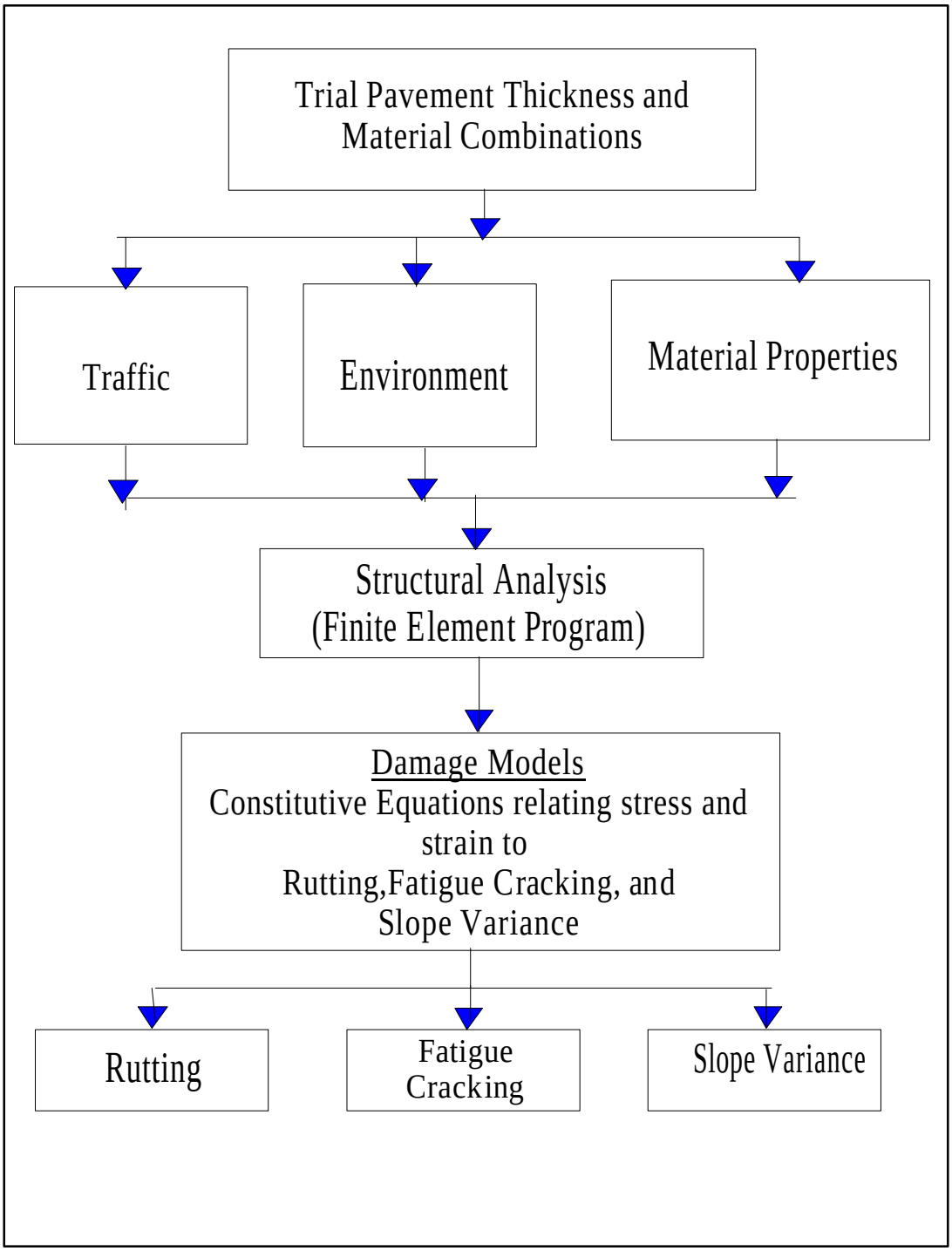

Figure 9
Simplified framework of FLEXPASS

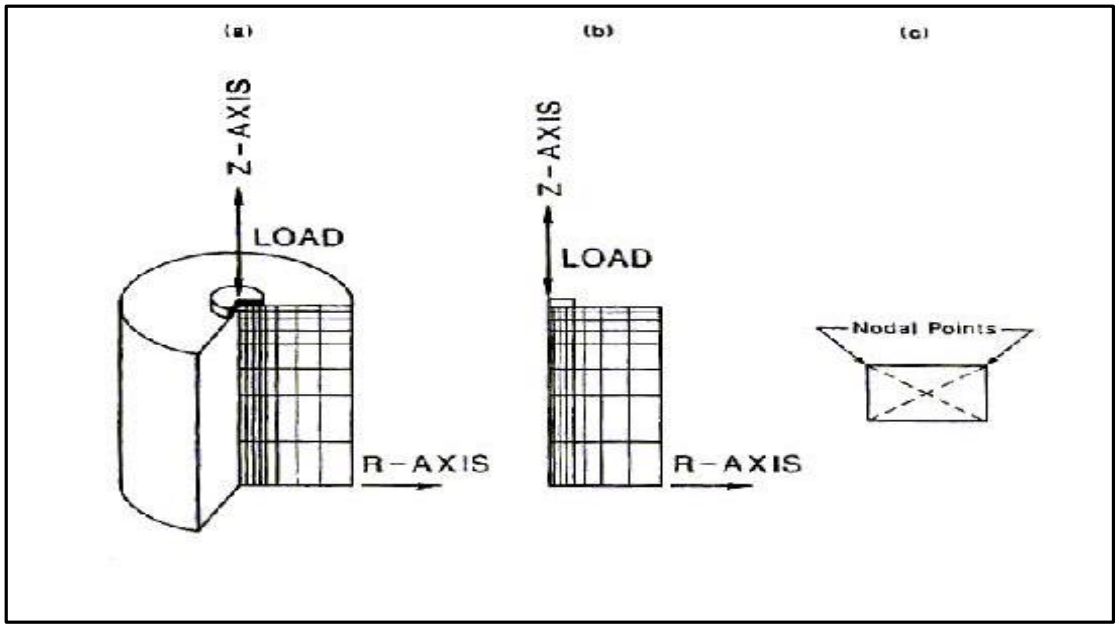

Figure 10
Finite element model in FLEXPASS: (a) 3-D view, (b) half-section, (c) typical element *[34]*

$$M_R = K_1(\Theta_3)^{K_2} \qquad (10)$$

if $(s_1 / s_3) < K_3$ and $s_3 > K_4$

where

Θ_3 is the bulk stress

K_1, K_2 are the material regression coefficients.

K_3 is the maximum allowable stress ratio, and

K_4 is the minimum horizontal compressive stress ratio.

3. Confining Pressure Dependent Modulus. This model describes the behavior of a granular material in which the modulus is a function of the confining pressure, s_3, and expressed as:

$$E_r = k_1(s_3)^{k_2} \qquad (11)$$

where K_1 and K_2 are regression constants determined from triaxial compression test results.

4. Deviator Stress Dependent Modulus. This model describes a soil material in which the modulus is a function of the deviator stress, and is represented by two intersecting, straight lines. The resilient modulus is described by:

$$E_r = X_1 + X_3[s_d - X_1], \text{ if } X_1 > (s_1 - s_3) \quad (12)$$

and

$$E_r = X_2 + X_4[s_d - X_1], \text{ if } X_1 < (s_1 - s_3) \quad (13)$$

In which

X_1 = Deviator stress (psi) at the break point

X_2 = Modulus value (psi) at the break point

X_3 = Slope of the left portion of the deviator stress-resilient modulus relationship

X_4 = Slope of the right portion of the deviator stress-resilient modulus relationship

Besides material modeling with nonlinear stress-dependent relations of pavement materials, a failure criterion based on the Mohr-Coulomb theory for granular materials and fine-grained soils is used to modify the calculated stresses so that they do not exceed the strength of the material. This criterion is accomplished in the program by setting numerical limits on the major and minor principal stresses which can be developed within the material layer. For the next iterative step, the modified stresses are then used in a stress-dependent resilient modulus relation, and then re-analyzed. A reasonable degree of convergence usually occurs in several iterations.

Criteria Selected to Define Failure in FLEXPASS Model

The structural deterioration of flexible pavement is usually related to two failure criteria: the load-induced cracking of the HMA layers and the development of ruts in the wheel paths. Rutting may occur in all layers and may be produced by both permanent vertical strain and lateral plastic flow in each layer. Fatigue cracking is considered the result of repeated flexural stresses causing tensile strains at the bottom of the asphalt base or binder course sufficient to initiate a crack and propagate it to the surface.

Rutting in Asphalt Pavement. Rutting is defined as a permanent deformation in and of the pavement layers or subgrade caused by consolidation or lateral movement of the

materials due to traffic loads. Pavement uplift may occur along the side of the rut. Rutting stems from the permanent deformation in any of the pavement layers or subgrade, usually caused by the consolidation or lateral movement of the materials due to traffic loads *[35]*. The biggest problem associated with rutting is water that collects in the ruts and can cause hydroplaning, a phenomenon in which fast moving vehicles lose contact between the tires and the pavement surface. As truck axle loads and tire pressures have increased in recent years, rutting has become a more serious problem.

In this project, non-linear elastic theory was used to predict stresses coupled with results from the laboratory repeated loading tests to predict the accumulated permanent strains of the pavement. The model for permanent deformation is based on an evaluation of the vertical resilient strain in each layer by the finite element method. It is also based on the fractional increase of total strains for each material layer of the pavement as determined by the permanent deformation characterization. The finite element analysis is used to take the nonlinear stress-strain behavior of the materials into account.

In general, the relationship between permanent strain and number of load repetitions is represented by a straightline on the log-log plot of permanent strain versus numbers of load repetitions. Two parameters that characterize this relationship are derived from the slope and the intercept of the straight line and used in the VESYS program *[19]*. However, it has been shown by other studies that a three-parameter, nonlinear equation more accurately describes asphalt composite behavior due to permanent deformation *[31], [34],[36]*. The three-parameter equation relating the permanent strain to loading cycles is given by *[34]:*

$$e_r = e_0 e^{-(r/N)b} \qquad (14)$$

where

e_r = permanent strain

N = number of load cycles

e_0, r, b = model parameters determined by regression from laboratory test data

These model parameters are used to define the permanent deformation properties of each structural layer in the test lanes. They are determined by fitting a curve that relates the cumulative permanent strain to the number of loading cycles from the data obtained from either creep and recovery tests or repeated load triaxial laboratory tests. Typical repeated load test results are shown as figure 11.

According to Tseng, the physical meaning of this equation can be explained by the graph in Figure 11 *[34]*. The parameter r is the scale factor on accumulated permanent strain; a larger r means that it takes a large number of load applications to reach a given level of permanent strain. The parameter b is a shape parameter for the permanent strain curve; values of b greater than 0.5 give a characteristic s-shape while values of b less than 0.5 produce a curve that gradually becomes asymptotic with x-axis.

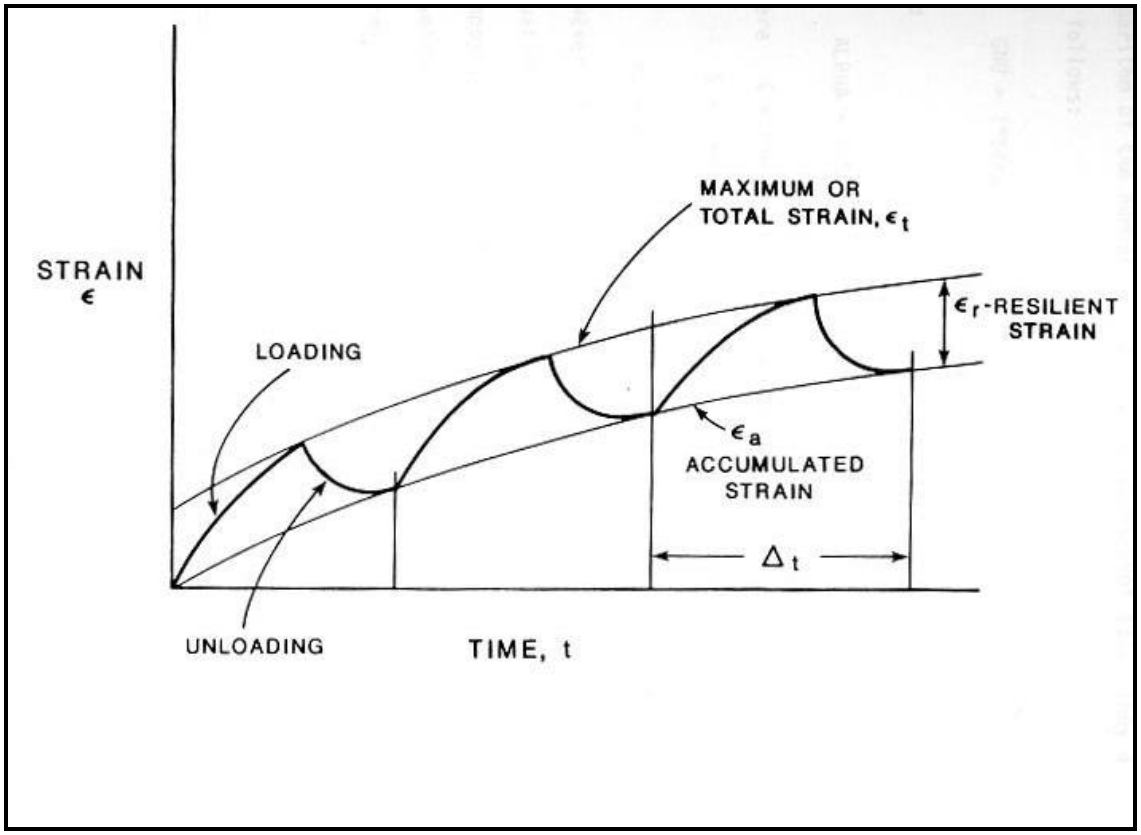

Figure 11
Typical repeated load test results

All curves pass through a common point where N = r, or at $e_a = e_0 * e^{-1} = 0.368e_0$. Using this equation, the relationship between strain and load cycles becomes non-linear and therefore more accurately represents the material behavior. According to the studies comparing measured deformations and predicted values elsewhere, this model has been found to be applicable to all flexible pavement materials, including HMA, granular bases, and subgrade soils *[37]*.

To calculate these three parameters for each ALF test material, in this study, repeated load compression tests were performed using the VESYS procedures for direct compression testing *[19]*. A plot of permanent strain versus loading cycles was made for each material tested to determine the shape of the curve and non-linear regression was used to calculate the three parameters. Details of the material permanent deformation characterization testing will be described later.

Fatigue cracking in Asphalt Pavements. Alligator or fatigue cracking is a series of interconnected cracks caused by fatigue failure of HMA layers under repeated loading. The cracking generally begins at the bottom of the HMA layer (or stabilized base) where tensile stress and strain are the highest under the wheel load. The cracks propagate to the surface initially as one or more longitudinal parallel cracks. After repeated traffic loading the cracks develop a pattern resembling chicken wire or alligator skin.

The presence of fatigue is an indication of the loss of structural (load-carrying) capacity in the pavement. Once cracking occurs at the bottom of the layer, it develops at an almost exponential rate.

Two different approaches are used to describe the fatigue behavior of HMA using laboratory test results *[34]:*

- The mechanistic approach.
- The phenomenological approach.

The mechanistic approach is based on the theory of fracture mechanics to arrive at the fatigue characterization. According to fracture mechanics theory, the stress intensity factor, K, controls the rate of crack propagation since K takes into account the effect of external loads and geometry which, in turn, intensifies the stresses near the crack tip. Also, fatigue life can be described as a process of crack initiation, propagation, and ultimate fracture *[34]:*

$$\frac{da}{dn} = A(\Delta K)^n \qquad (15)$$

where

A and n are the fracture parameters, and

ΔK is the difference of the stress intensity factor that occurs at the crack during one load pass

The number of load cycles to failure, N_f, is then expressed by *[34]:*

$$N_f = \int_{C_0}^{C_f} \frac{da}{A(\Delta K)^n} \quad (16)$$

where C_0 is initial crack length, and C_f is final crack length.

The phenomenological approach is an empirical approach in which the fatigue characteristics of asphalt mixes are described by relationships between initial stress or strain and the number of load repetitions to failure. The fatigue life is measured by laboratory testing a beam under controlled stress or controlled strain conditions or by testing a cylindrical sample loaded repeatedly along its vertical diameter.

In this project, the phenomenological regression approach was used to describe fatigue of the ALF test lane materials. This approach is the most common method for analyzing highway materials *[36]*. The fatigue cracking of a pavement layer is modeled by *[34]:*

$$N_f = K_1\left(\frac{1}{e}\right)^{K_2} \quad (17)$$

where

N_f = number of load applications to failure

e = tensile strain at the bottom of the asphalt layer

K_1, K_2 = parameters of the fatigue model

This equation describes a straight line on a log-log plot of cycles to failure versus bending strain, where log K_1 is the intercept of the y-axis, and $-K_2$ is the slope of the straight line. K_1 and K_2 are influenced by such factors as the type of load, dimensions of the test specimen, loading rate, test type, temperature, and the properties of the mix, including air voids, aggregate gradation and type, asphalt content and viscosity, etc. K_1 and K_2 of each HMA material is determined by the laboratory fatigue testing using the indirect tensile fatigue test at constant strain conditions *[36]*. This approach provides a reasonably simple procedure that has gained wide acceptance.

Slope Variance in Asphalt Pavements. Slope variance is defined as the variance of the slopes along the longitudinal profile of the roadway. A method to calculate the slope variance is based on the assumption that slope variance is a function of the spatial variations in the properties and thickness of the layer materials *[34]*. From this assumption, an auto correlation function of the permanent surface deformation is assumed. Kenis expressed the auto correlation function in terms of pavement deflection

response and material variability and showed that slope variance is equal to the negative second derivative of the auto correlation function *[19]*. The expression for the slope variance in terms of the variation of the load deflection response, rutting, and variance of rutting can be developed as *[34]:*

$$E[sv] = \frac{2B}{C^2}\,\mathrm{var}[d_a] \tag{18}$$

where

$E[sv]$ = expected value of slope variance,

$\mathrm{var}[d_a]$ = variance of rut depth, and

B and C = roughness properties.

Present Serviceability Index. The present serviceability index (PSI) as an indicator of pavement performance was developed at the AASHO Road Test. This index was predicted from measurements taken on the pavement surface, including rutting, slope variance, cracking, and patching. PSI was predicted from the following equation *[19]:*

$$PSI = 5.03 - 1.91\log(1+sv) - 1.38(d_a)^2 - 0.01\sqrt{\bar{c}+p} \tag{19}$$

where p is the area of patching in square feet per 1000 square feet.

$\bar{c}$ is the cracked area in square feet per 1000 square feet.

sv is the slope variance.

d_a is the average rut depth, in.

Laboratory Testing of ALF Pavement Materials

As mentioned earlier, the material parameters must be defined for the rutting and the fatigue prediction models used in the FLEXPASS analysis. Tests performed to measure these properties include:

- Repeated Load Compression Test (Permanent Deformation Prediction)
- Repeated Loading Indirect Tension Test (Fatigue Prediction)

Four materials were tested:

- T8WC (Conventional Type 8 Wearing Course)

- T8WC-PRM (PRM-HMA Type 8 Wearing Course)
- Base (Conventional Base Course with AC-30 asphalt)
- Base PRM (PRM-HMA Base Course).

It should be noted that previous testing showed that the Type 8 binder course properties were very similar to those of the Type 8 wearing course. As a result, only the wearing course was tested and the resulting properties were assigned to the combined wearing and base course thickness in all the modeling studies. The tests on each of the four mixes were performed to determine the properties of the materials at a range of temperatures and typical loading rates. As a result the seasonal temperature changes and different axle loads that occurred during the ALF testing were simulated. Each test has been described, so only the typical test results for each of the four mixes tested will be discussed. All of the specimen preparation and testing were conducted in the Engineering Materials Characterization and Research Facility (EMCRF) at LTRC.

The specimen preparation and testing were performed to obtain the material parameters needed in the performance prediction models so that a realistic comparison could be made between the performance of the PRM-HMA and that of the conventional HMA. The optimal position of PRM-HMA in the pavement structure was also evaluated. Since the asphalt mixtures were plant produced, laboratory mixing was not required. Specimens used to develop the material characteristics used in performance predictions were prepared using the Superpave Gyratory Compactor (SGC) from plant produced materials.

Design of the Experiments. All specimens were cylindrical in shape. There were two types of specimen sizes: 4 in. (101-mm) in diameter by 6 in. (150-mm) in height made for Repeated Load Compression (RLC) Testing, and 4 in. (101-mm) in diameter by 2 ½-in. (63-mm) in height made for Indirect Tensile Fatigue (ITF) Testing.

The Repeated Load Compression (RLC) Test was conducted at three temperatures: 40, 77, and 104°F (4,77, and 40°C). Three replicates were tested for each combination of material and temperature.

Indirect Tensile Fatigue (ITF) Tests were conducted at two temperatures: 77°F (25°C), and 104°F (40°C). Three replicates were tested for each combination of material and temperature.

Table 7 shows the tests performed for each mixture.

Table 7
Test factorial for material performance tests

Tests	Sample Size, D X H, in. (mm)	Test Temperature, °F (°C)	Mixtures			
			T8WC (PAC 40)	T8WC (PRM)	Base (AC-30)	Base (PRM)
ITF	4 X 2 ½ (101 x 63)	77,104 (25, 40)	3, 3*	3, 3	3, 3	3, 3
RLC	4 X 6 (101 x 150)	40, 77, 104 (4, 25,40)	3, 3,3	3, 3,3	3, 3,3	3, 3,3

***The number represents the replicas for each combination of temperature and mixture.

Test Results and Analysis. A plot of permanent strain versus load cycles was made for was made for the test results from each specimen to determine the shape of the curve and if the three-parameter equation suitably described the material behavior.

Because the operator performing the tests was relatively inexperienced, there was significant operator error in the test data. To minimize this influence, each test result was reviewed and the consistent test results were averaged for each material at each of the three test temperatures.

A Non-Linear regression procedure (NLIN) from the S.A.S package was used to develop the test parameters for the average test result for each material at each temperature. The NLIN procedure produces the least square or weighted least-squares estimates of the parameters of a nonlinear model. The procedure uses an iterative process in which the form of the regression expression is selected, the derivatives of the model with respect to the parameters are specified, and an initial starting value for each parameter is input. The modified Gauss-Newton method was selected for this analysis. In the Gauss-Newton method, the residuals are regressed onto the partial derivatives of the model with respect to the parameters until the iterations converged. The iterations converge if

$$(SSE_{i-1} - SSE_i)/(SSE_i + 10^{-6}) < 10^{-8}$$

where i is the number of iterations.

Tables 8 through 11 contain the predicted permanent deformation parameters for each material at each test temperature.

Table 8
Predicted permanent deformation parameters for type 8 wearing course (T8WC) and type 8 binder course (T8BC) with PAC-40

Temperature, °F (°C)	e_0/e_r	r	b	Log(e_0/e_r)	Log r	Log b
40 (4)	0.63	89.64	1.3474	-0.20066	1.952502	0.129497
77 (25)	1.77	144.6	0.5223	0.247973	2.160168	-0.28208
104 (40)	21.85	5.52E+10	0.0849	1.339451	10.74194	-1.07109

Table 9
Predicted permanent deformation parameters for T8WC with PRM

Temperature, °F (°C)	e_0/e_r	r	b	Log(e_0/e_r)	Log r	Log b
40 (4)	0.66	315.4	0.4165	-0.18046	2.498862	-0.38038
77 (25)	1.8	410.6	0.3284	0.255273	2.613419	-0.4836
104 (40)	253.2	1.01E+17	0.0583	2.403464	17.00432	-1.23433

Table 10
Predicted permanent deformation parameters for a conventional base with AC-30

Temperature, °F (°C)	e_0/e_r	r	b	Log(e_0/e_r)	Log r	Log b
40 (4)	1.11	164.2	0.81	0.045323	2.215373	-0.09151
77 (25)	1	38.326	0.6116	0	1.583493	-0.21353
104 (40)	196.5	1.49E+21	0.0467	2.293363	21.17319	-1.33068

Table 11
Predicted permanent deformation parameters for base with PRM

Temperature, ^{o}F (^{o}C)	e_0 / e_r	r	b	Log(e_0 / e_r)	Log r	Log b
40 (4)	1	304.8	0.3513	0	2.484015	-0.45432
77 (25)	1.5	27.9573	0.3772	0.176091	1.446495	-0.42343
104 (40)	50	1.84E+17	0.0537	1.69897	17.26482	-1.27003

ALF Loading History and Field Measurements

ALF Loading History

To simulate highway traffic, the ALF loads were applied only in one direction and were normally distributed about a 32-inch (813-mm) wheel path. The magnitude of the ALF loading varied with number of loading plates. At the beginning of the test, a 9.75-kip (43 kN) load was applied through dual-tires with tire pressure maintained at 105-psi (724-kPa). The initial 9.75-kip (43-kN) load was applied for a period of time and then the load was increased in increments of 2,300-pounds (10.2-kN), at the intervals noted in Table 12, at the same tire pressure until each test lane failed. The total traffic applied to test lanes 2-1 and 2-3 was 800,000 passes while lane 2-2 received 850,000 passes as shown in Table 12.

The loading was applied alternatively between the test lanes in 25,000 pass increments in an attempt to minimize the relative environmental effects occurring during the loading period. Rutting of 0.50 in. (12.7-mm) or a decrease in PSI to 2.5 were defined as failure conditions for pavement.

Field Measurements

Field measurements included the periodic collection of cracking, transverse and longitudinal profile, deflection data, and temperatures. The ALF loading was stopped periodically for maintenance, and surface measurements were made at those times.

Each of the lanes had the transverse profile measured after each increment of 25,000 load

Table 12
ALF passes applied to test lanes

No. of Passes x 1000	Total Load, Lbs. [1](kN)	ESAL Factor	ESALs	Cumulative ESALs	Date Load First Applied
0 - 400	9,750 (43.0)	1.377	550,800	550,800	3/5/99
400 - 500	12,050 (53.6)	3.213	321,300	872,100	10/4/99
500 - 650	14,350 (63.6)	6.463	969,450	1,841,550	12/6/99
650 - 750	16,650 (74.0)	11.713	1,171,300	3,012,850	4/14/00
750 - 800	18,950 (84.2)	19.655	982,750	3,995,600	10/9/00
800 - 850	21,250[2] (94.4)	31.079	1,553,950	5,549,550	12/18/00

[1]Each addition load increment represents 2,300 pounds (10.2-kN)
[2]Load applied only to Lane 2-2, PRM Base

passes. For the transverse profile, eight profile measurement stations were located at 4 ft. (1.22-m) intervals along the 35 ft. (10.67-m) test lane. The profile data were secured using the ALF profilograph, which consists of a linear variable differential transformer (LVDT) mounted on a metal carriage. It moves transversely across the pavement on a metal frame. The metal frame can be positioned along the pavement section between two rails mounted on the pavement surface, outside the trafficked area. A rut depth is calculated from each transverse profile.

Deflection testing was conducted on a periodic basis using the falling weight deflectometer (FWD) and the Dynaflect. The FWD data were used to backcalculate the moduli of each layer of the test sections. Applying an impulse force generated from two mass assemblies in which the falling weight was dropped onto a second weight/buffer combination created the deflection measurement. The measurements with each device were performed on the centerline of the loading path of each pavement test section at eight stations spaced at intervals of 4 ft. (1.22-m) along the centerline.

Studies to Compare Analytical Predictions with Field Measurements

All data, measurements and observations obtained during the ALF field testing and lab material testing were evaluated to examine and compare the relative strength and performance characteristics of the test lanes. In addition, computer performance predictions were conducted by using the material characterization test data to predict performance of the test lanes under the same environmental conditions existing during the ALF field tests. The mechanistic-empirical method of predicting performance is based on mechanics of materials principles that relate input, such as wheel load, to an output or pavement response, such as stress or strain. The pavement response values are used to predict distresses. A finite element software package-- FLEXPASS was used to analyze the pavement responses and to predict performance. The performance prediction included rutting, fatigue cracking, and PSI. The analytical results were compared with the ALF field measurements. In addition to the FLEXPASS predictions, ABAQUS-predicted strains and deflections were compared to field measurements and these comparisons provide an indication of the accuracy of the 3-D modeling techniques.

Evaluation of Structural Coefficients for PRM Surface and Base Mixes

Three methods were used to calculate the structural numbers (SN) for the three ALF experiment 2 test lanes:

1. Backcalculation of SN using the AASHTO flexible pavement design equation,

2. Calculation using results from the Dynaflect and an analysis procedure used by the Louisiana Department of Transportation and Development, and

3. Calculation using results from the Falling Weight Deflectometer (FWD) and a procedure reported by Rohde*[38]*.

SN Using AASHTO Equation. **The AASHTO flexible pavement design equation is:**

$$\text{Log } W_{18} = z_R * s_o + 9.36 \text{ Log } (SN+1) - 0.2 + \{\text{Log } [(P_i - P_t)/2.7]/[0.4 + 1094/(SN+1)^{5.19}]\} + 2.321 \text{ Log } M_R - 8.07 \quad (20)$$

Where:

W_{18} = No. of 18-kip (80-kN) equivalent single axle loads expected in the design lane during the design life of the lane

z_R = Standard normal deviate, z, corresponding to the Reliability chosen for the traffic variation

s_o = Standard deviation representing the total variation in construction and traffic prediction for the project. In Louisiana, s_o has been selected as 0.47 for flexible pavements

SN = AASHTO structural number representing the combined strength of the total pavement structure

P_i = Initial Present Serviceability Index (PSI) of the pavement immediately after construction

P_t = Terminal Present Serviceability Index of the pavement at the time when a major rehabilitation normally occurs

M_R = Resilient modulus of the subgrade soil, psi

The AASHTO equation was solved for SN using data collected at the ALF site for each of the test lanes, such as traffic and resilient modulus of the subgrade soil from testing performed at the LTRC laboratories. The serviceability data in the equation was taken from the FLEXPASS predictions of performance. The reliability chosen for this analysis was 95 percent, which is appropriate for Interstate type highways. The pavement layer thicknesses constructed on these test lanes are typical of high volume roadways. Since SN occurs twice in the equation, an iterative procedure was used to solve for SN.

SN from Dynaflect Data. The Dynaflect is a device used to apply light loads, 2,000 lbs (8.9 kN), to a pavement structure and to measure the deflection response of the pavement to the load using sensors at the load and spaced along the road surface. These measurements were performed approximately every 25,000 applications of the ALF axle load. Eight measurements were taken in each test lane at approximately every 4 ft. (1.22 m) along the loaded area. After the deflection measurements were taken, an analysis was performed in which pavement characteristics including SN were calculated. These data were provided by the LTRC team at the ALF site and will be presented in the discussion section of this report.

SN from Falling Weight Deflectometer Data. The falling weight deflectometer (FWD) is a device used to apply a heavy load, approximately 9,000 lbs (40 kN) or higher, to a pavement structure and to measure the deflection response of the pavement to the

load using sensors at the load and spaced along the road surface. These measurements were also performed using the same protocol as with the Dynaflect. The data was collected by the LTRC team at the ALF site and analyzed using a procedure described by Rohde*[38]*.

The peak deflection produced by the load from a FWD is a combination of the deflection in the subgrade soil and compression of the layers in the pavement structure. In 1983, Irwin *[39]* suggested that about 95 percent of the deflection at the surface of a roadway is contained within the region defined by a line drawn from the edge of the load plate and 34^o from the horizontal surface of the road as shown in figure 12. Irwin assumed that the surface deflection measured at an offset of 1.5 times the pavement thickness originates completely in the subgrade. By comparing this deflection with the peak deflection, an index associated with the magnitude of deflection occurring within the pavement structure could be defined:

$$SIP = D_o - D_{1.5Hp} \quad (21)$$

where:
SIP = Structural Index of the Pavement Structure
D_o = Surface deflection measured under the FWD load
$D_{1.5Hp}$ = Surface deflection, measured or interpolated, at an offset of 1.5 times Hp from the center of the plate where the FWD load is applied
Hp = Total Pavement Thickness

To investigate the hypothesis that SIP is correlated with pavement stiffness and subsequently to structural number, a large number of pavements were analyzed using elastic-layered theory and a series of relationships developed between various pavement properties and deflections under load. The best relationship was:

$$SN = 0.4728*[(SIP)^{-0.4810}]*Hp^{0.7581} \quad (22)$$

where:
SN = Structural Number
SIP = Structural Index, micrometers
Hp = Total Pavement Thickness, millimeters

Rohde *[38]* investigated the use of backcalculated moduli, dynamic cone penetrometer results, surface deflection analysis, and shape of the deflection bowls from AASHTO

methods 1 and 2 in addition to the equation above to determine which method provided the best estimate for structural number. Rohde concluded that the above equation provided results that were consistent and correlated highly with AASHTO Method 1 but that the above equation was simpler to use. Analysis of the ALF test section data using the above procedure is provided in the discussion section of this report.

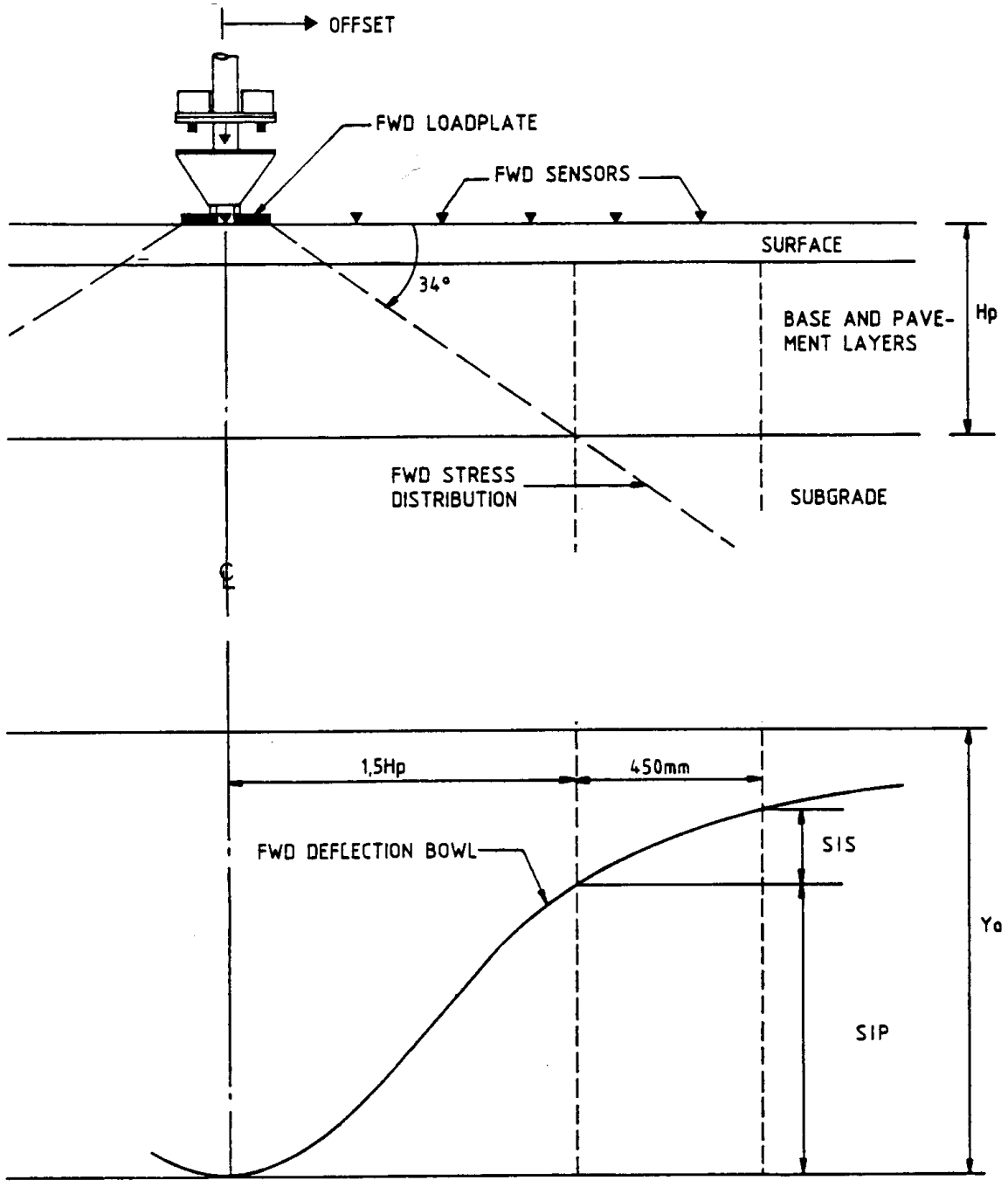

Figure 12

Stress distribution and measured deflection basin under a FWD load ***[38]***

DISCUSSION OF RESULTS

Laboratory Test Results

A standard statistical procedure, One Way Analysis of Variance (ANOVA), was used to test if the mean values of the engineering properties were significantly different between each group. A 95 percent confidence level was used to analyze the test results. The ANOVA places sample averages into groups by determining which averages are statistically equal. Groups are designated by letters "A", "B", "AB", etc. Group "A" has a mean that is statistically higher than group "B" and so forth. A designation of "AB" shows that the average can be placed into either its corresponding statistical ranking group "A" or "B".

Indirect Tensile Resilient Modulus (M_R)

Indirect tensile resilient modulus (M_R) represents the elastic property of the HMA at the test temperature. Table 13 and figure 13 present the mean indirect tensile resilient modulus (M_R) test results at 40, 77 and 104 ^oF (4, 25 and 40^oC). As expected, the values of M_R decrease as temperature increases. There was no significant difference between the conventional type 8 wearing course mix and the PRM-HMA wearing course mixture at any temperature. Neither was there a significant difference between the conventional base course mix and the corresponding base course mix containing PRM binder at any temperature. In Table 13, only the type 8 wearing course properties are shown because the binder course and wearing course properties are the same.

Table 13
Statistical grouping of indirect tensile resilient modulus (M_R)

Temperature	Engineering Property	Mixtures			
		T8 WC	T8 WC-PRM	Base	PRM Base
4^oC (40^oF)	M_R (GPa)	4.37	4.31	4.33	4.39
	Ranking	A	A	A	A
25^oC (77^oF)	M_R (GPa)	3.20	3.09	3.81	3.31
	Ranking	A	A	A	A
40^oC (104^oF)	M_R (GPa)	1.97	1.69	2.20	2.24
	Ranking	A	A	A	A

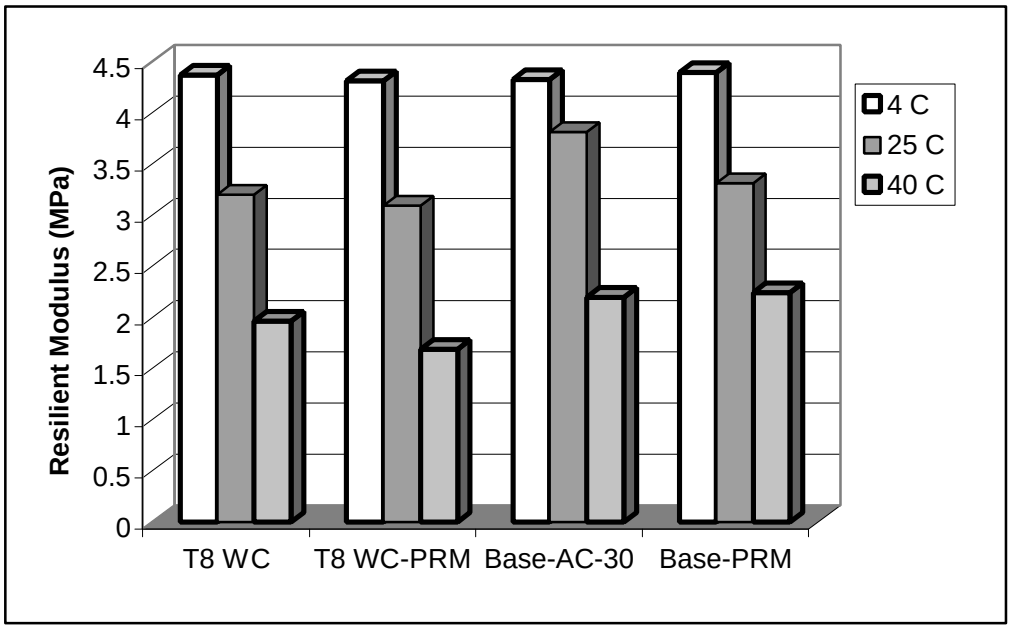

Figure 13
Indirect tensile resilient modulus (M_R) test results

Indirect Tensile Strength (ITS)

Table 14 presents the averages of the indirect tensile strength (ITS) and the corresponding strain at failure and the toughness index (TI). There was no significant difference between the conventional mixtures and PRM mixtures in either wearing course or base course groups.

Table 14
Statistical grouping of indirect tensile strength (ITS) results

Engineering Property	Mixtures			
	T8WC	T8WC-PRM	Base	PRM Base
ITS (MPa)	1.40	1.25	1.76	1.88
Ranking	A	A	A	A
Strain at Failure	0.56	0.55	0.41	0.39
Ranking	A	A	A	A
TI	0.51	0.55	0.36	0.28
Ranking	A	A	A	A

Indirect Tensile Creep (IT-CRP) Results

In the indirect tensile creep (IT-CRP) test, lower creep slope and longer time to failure are desired for rut resistance. Table 15 presents the results from the indirect tensile creep test at 77°F (40°C). The PRM-HMA base course mix had a significantly lower creep slope and longer time to failure than the conventional base course. However, the slopes and time to failure of PRM-HMA and conventional wearing course mixes were statistically similar. The results from this test indicated that base course mixture with powdered rubber modified binder had improved rut resistance properties when compared to the corresponding conventional mixture.

Table 15
Statistical grouping of indirect tensile creep (IT-CRP) results

Engineering Property	Mixtures			
	T8 WC	T8 WC-PRM	Base	PRM Base
Creep Slope	0.40	0.38	0.40	0.32
Ranking	A	A	A	B
Time to Failure, min.	1040	774	1451	>3600
Ranking	A	A	A	B

Axial Creep (AX-CRP) Test Results

Table 16 presents the statistical mean and grouping of the axial creep test results. It should be noted that the variability in results from this test is high. As a result, the distributions of data are broad and the statistical tests were unable to distinguish between the means. The PRM-HMA mixtures showed similar results from this test compared to the corresponding conventional mixtures. The average values of creep stiffness of all four mixes were within the range as defined by the Texas specification *[26]*. The creep slope for all mixes except the base were outside the Texas specification of $<3.5x10^{-8}$, and the permanent strain of the conventional Louisiana Type 8 wearing course mixture was outside the Texas specification of $<5.0x10^{-4}$.

Frequency Sweep at Constant Height (FSCH) Results (60 ºC)

Figures 14 and 15 present the dynamic shear modulus (G*) and shear phase angle (*) versus frequency from the frequency sweep at constant height (FSCH) test. Table 17 shows the mean of the G* and * at 0.01 Hz and 10 Hz and their statistical grouping. The PRM-HMA wearing course mixture had higher dynamic shear modulus (G*) values than the conventional Type 8 wearing course mixture at all frequency levels, although their differences were not statistically significant (table 17) because of the higher coefficient of variation of the PRM Type 8 wearing course.

Table 16
Statistical grouping of axial creep (AX-CRP) results

Engineering Property	Mixtures				Texas Spec
	T8 WC	T8 WC-PRM	Base	PRM Base	
Stiffness (MPa)	60.5	60.8	64.4	64.3	> 44.1
C.V. (%)	5.2	5.3	13.9	8.7	
Ranking	A	A	A	A	
Creep Slope $x10^{-8}$	9.5	5.4	1.9	6.3	< 3.50
C.V. (%)	39.9	22.5	17.9	10.2	
Ranking	A	A	A	A	
Perm Strain $x10^{-4}$	5.15	4.11	2.57	3.81	< 5.0
C.V. (%)	40.1	24.1	31.4	25.8	
Ranking	A	A	A	A	

Table 17
Statistical grouping of FSCH test results at 104°F (60°C)

Engineering Property	Mixtures	
	T8 WC	T8 WC-PRM
G* at 0.01 Hz (MPa)	13.5	14.8
C.V. (%)	9.3	24.3
Ranking	A	A
G* at 10 Hz (Mpa)	62.5	95.4
C.V. (%)	0.3	41.1
Ranking	A	A
* at 0.01 Hz (°)	28.5	29.6
C.V. (%)	23.1	34.7
Ranking	A	A
* at 10 Hz (°)	43.2	43.6
C.V. (%)	2.9	8.4
Ranking	A	A

Repetitive Shear at Constant Height (RSCH) Results at 104°F (60 °C)

Figure 16 presents the results of Superpave repetitive shear at constant height (RSCH) test. The permanent strains for all mixtures at 5,000 cycles were below the specified value of 5 percent. However, the conventional base and PRM-HMA wearing course mixtures exhibited higher average permanent strains than did the PRM base and conventional Type 8 wearing course mixtures, respectively. However, a statistical analysis revealed no significant differences in permanent deformation between the PRM

wearing and conventional wearing course mixtures or the PRM base and conventional base mixtures.

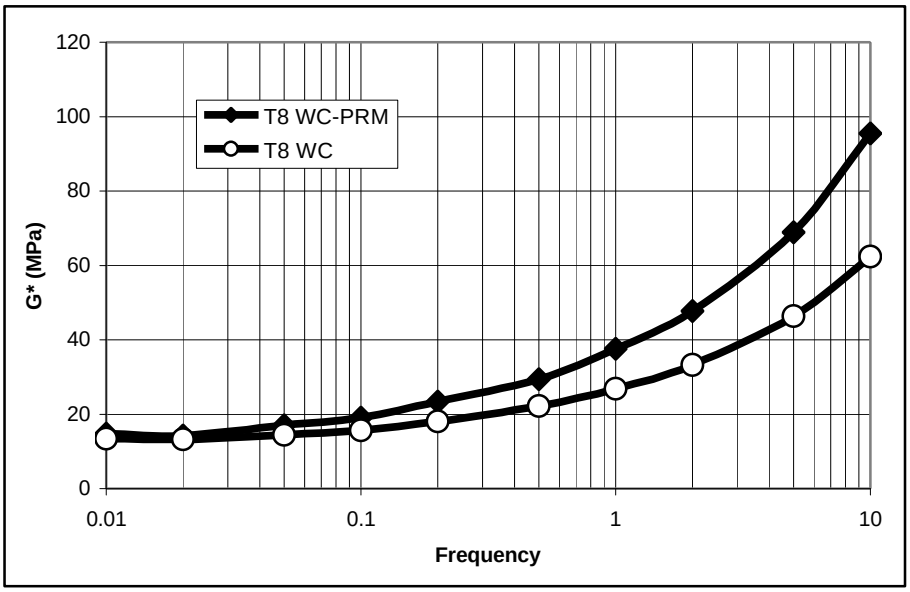

Figure 14
Dynamic shear modulus of FSCH test

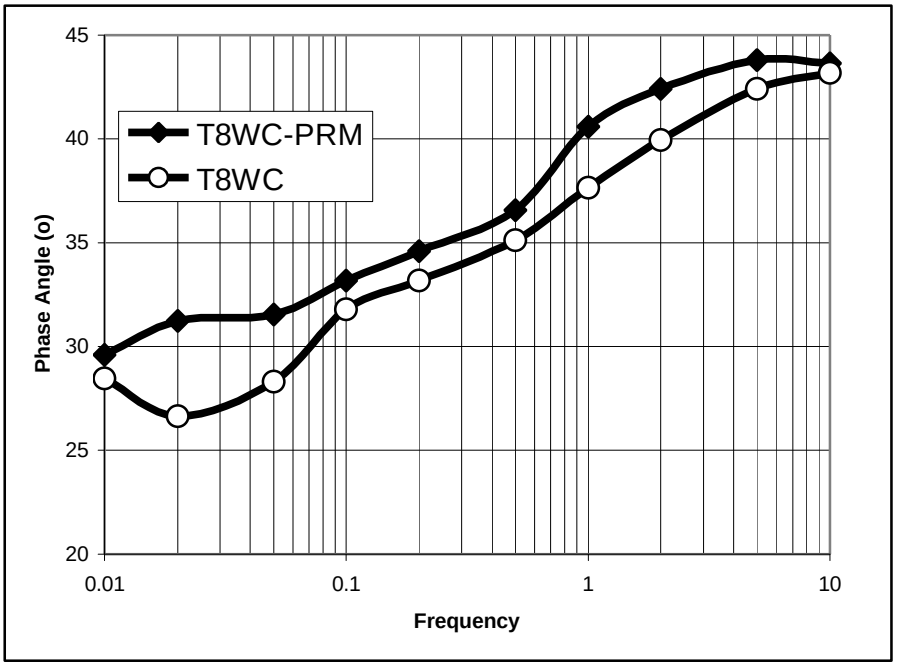

Figure 15
Shear phase angle of FSCH test

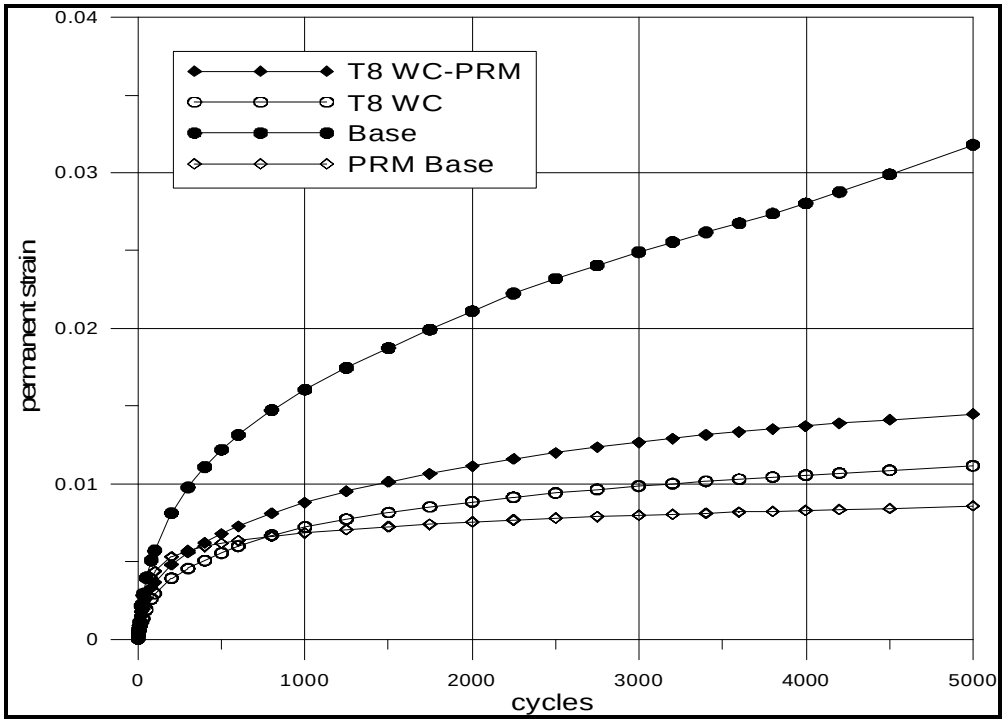

Figure 16
Permanent strains of RSCH test

ALF Field Experiment Results

Observed Field Rutting

Figure 17 shows the transverse profile of the test lanes at the end of ALF loadings (table 18) as measured from a stringline across each lane to the surface where a trench was cut. The stringline extended from one edge of the test lane across the lane to the other side. The trench was cut at the end of testing in order to determine how much rutting occurred in each layer of the pavement structure. The data in Table 18 shows that there may have been some slight horizontal shear displacement in the HMA of lanes 2-1 and 2-3 since the displacements at both ends of the 8 ft. (2.44-m) straight edge showed some vertical movement. Since a transverse profile of each test lane was not taken before testing, a plane section profile was assumed to be constructed.

Measurements were taken during ALF loading to define the transverse profile for each station and to calculate the average rut depth of the test lanes. For each test lane,

transverse measurements were taken at eight stations over a length of 30 ft. (9.14 m) within the 38 ft. (11.58 m) loading area. Eight transverse profiles were measured after every 25,000 ALF load applications. The average of these eight rut depth measurements was reported and used to compare with the FLEXPASS predictions and is included in tables 19 through 21. Figure 18 shows the average rut depths versus accumulated 18-kip (80-kN) ESALs for all three test lanes. The results showed that rutting began very early for lane 2-3 (control lane) with 0.12 inch (0.30 cm) rut depth at about 35,000 ESALs, while the other two lanes showed very little rutting (around 0.03 inch [0.08 cm]) at this loading stage. The rutting developed at a much faster rate in lanes 2-3 and 2-1 than in lane 2-2. All three lanes experienced a uniform rate of rutting until around 500,000 ESALs when the rutting rate reduced dramatically in all lanes. During the first half million ESALs, rutting development in lane 2-3 was the fastest and the rut depth was the largest, whereas rutting development in lane 2-2 was the slowest and the rut depth was about 35 percent lower than the other two lanes. All three lanes showed little additional rut depth development between 500,000 and 2,100,000 ESALs. During this loading period, the wheel load increased from 9,750 to 14,350 lbs. (43.29 to 63.71 kN). After that, the rut development began to increase again until the end of loading. The final measured rut depth for lane 2-1 and lane 2-3 were 0.56 and 0.55 in. (14.22 and 13.97 mm) respectively, both were about 55 percent higher than the rutting of lane 2-2 (0.36 inch [0.89 cm]).

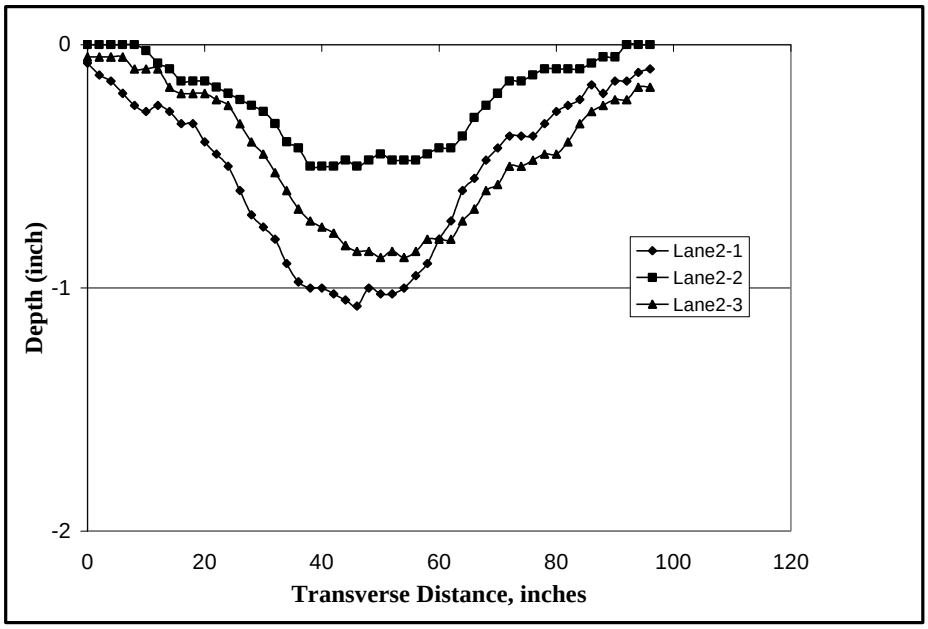

Figure 17
Transverse profile for all test lanes at the end of ALF testing as measured from a stringline

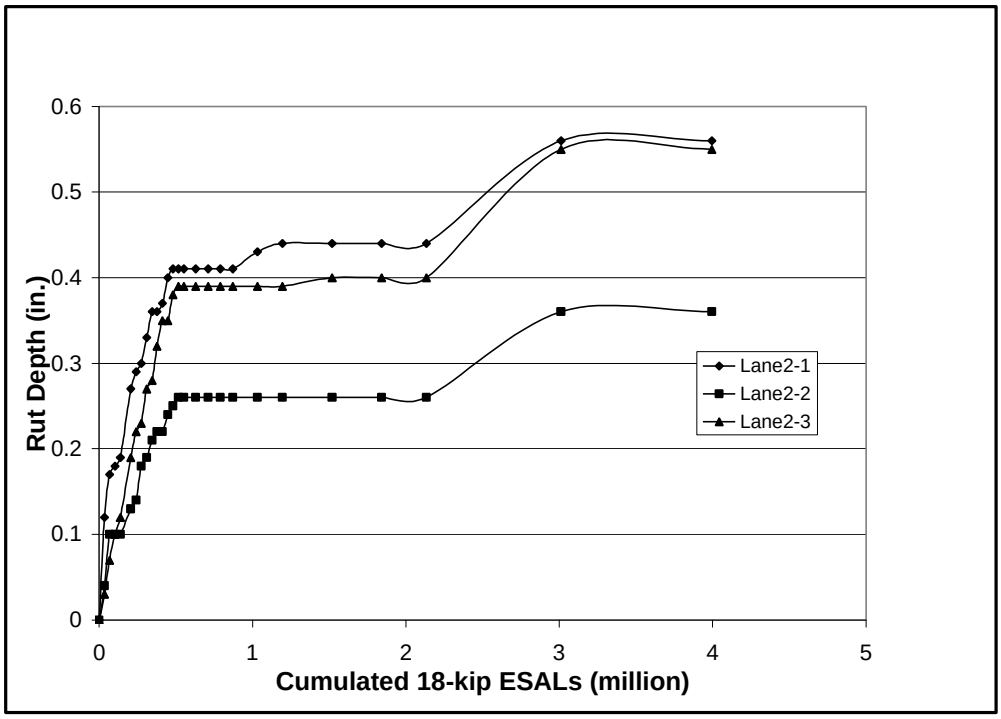

Figure 18
Observed rut depth versus cumulative 18-kip (80 kN) ESALs for test lanes

Figure 19 presents the average rut depth for all eight stations as well as the calculated variation in rut depth measurements versus load cycles of lane 2-1 (PRM-HMA in the wearing course) and lane 2-3 (conventional mixes). The hatched area represents the 95 percent confidence levels for measured rut depth based on the t-test. Notice that the data for lane 2-3 is completely contained within the data for lane 2-1. Similarly, Figure 20 presents the rut depths of lane 2-2 (PRM-HMA in the base course) and lane 2-3 (conventional mixes). It appeared that at 95 percent confidence, the rut depth of lane 2-2 was significantly smaller than both lane 2-1 and lane 2-3 (with little overlap of the hatched areas between lanes 2-2 and 2-3). However, the rut depth of lane 2-1 and lane 2-3 were similar (majority of the hatched areas were overlapped). This observation was consistent with the laboratory material characterization which showed that the wearing course mixes with and without powdered rubber were similar, whereas, the base course mixes with powdered rubber had better rut resistance than those mixes with no powdered rubber.

Observed Fatigue Cracking

The pavement surface was examined every 25,000 passes for evidence of cracking. There were no observed fatigue cracks in any of the lanes during the entire ALF loading history. In fact, no cracks of any type occurred in any of the test lanes.

Table 18
Transverse profile across each test lane at the end of ALF loading at a trench cut in each test lane

Transverse Distance, in(mm)	Lane2-1 in(mm)	Lane2-2 in (mm)	Lane2-3 in(mm)	Transverse Distance, in(mm)	Lane2-1 in(mm)	Lane2-2 in(mm)	Lane2-3 in(mm)
0	-0.075 (-1.90)	0	-0.05 (-1.27)	48 (1219)	-1.00 (-25.4)	-0.475 (-12.06)	-0.85 (-21.59)
2 (51)	-0.125 (-3.18)	0	-0.05 (-1.27)	50 (1270)	-1.025 (-26.04)	-0.45 (-11.43)	-0.875 (-22.22)
4 (102)	-0.15 (-3.81)	0	-0.05 (-1.27)	52 (1321)	-1.025 (-26.04)	-0.475 (-12.06)	-0.85 (-21.59)
6 (152)	-0.2 (-5.08)	0	-0.05 (-1.27)	54 (1372)	-1.00 (-25.4)	-0.475 (-12.06)	-0.875 (-22.22)
8 (204)	-0.25 (-6.35)	0	-0.1 (-2.54)	56 (1422)	-0.95 (-24.13)	-0.475 (-12.06)	-0.85 (-21.59)
10 (254)	-0.275 (-6.98)	-0.025 (-0.64)	-0.1 (-2.54)	58 (1473)	-0.9 (-22.86)	-0.45 (-11.43)	-0.8 (-20.32)
12 (305)	-0.25 (-6.35)	-0.075 (-1.90)	-0.1 (-2.54)	60 (1524)	-0.8 (-20.32)	-0.425 (-10.80)	-0.8 (-20.32)
14 (356)	-0.275 (-6.98)	-0.1 (-2.54)	-0.175 (-4.44)	62 (1575)	-0.725 (-18.42)	-0.425 (-10.80)	-0.8 (-20.32)
16 (406)	-0.325 (-8.26)	-0.15 (-3.81)	-0.2 (-5.08)	64 (1626)	-0.6 (-15.24)	-0.375 (-9.52)	-0.725 (-18.42)
18 (457)	-0.325 (-8.26)	-0.15 (-3.81)	-0.2 (-5.08)	66 (1676)	-0.55 (-13.97)	-0.3 (-7.62)	-0.675 (-17.14)
20 (508)	-0.4 (-10.16)	-0.15 (-3.81)	-0.2 (-5.08)	68 (1727)	-0.475 (-12.06)	-0.25 (-6.35)	-0.6 (-15.24)
22 (558)	-0.45 (-11.43)	-0.175 (-4.44)	-0.225 (-5.72)	70 (1778)	-0.425 (-10.80)	-0.2 (-5.08)	-0.575 (-14.60)
24 (610)	-0.5 (-12.70)	-0.2 (-5.08)	-0.25 (-6.35)	72 (1829)	-0.375 (-9.52)	-0.15 (-3.81)	-0.5 (-12.7)
26 (660)	-0.6 (-15.24)	-0.225 (-5.62)	-0.325 (-8.26)	74 (1880)	-0.375 (-9.52)	-0.15 (-3.81)	-0.5 (-12.7)
28 (711)	-0.7 (-17.78)	-0.25 (-6.35)	-0.4 (-10.16)	76 (1930)	-0.375 (-9.52)	-0.125 (-3.18)	-0.475 (-12.06)
30 (762)	-0.75 (-19.05)	-0.275 (-6.99)	-0.45 (-11.43)	78 (1981)	-0.325 (-8.26)	-0.1 (-2.54)	-0.45 (-11.43)
32 (813)	-0.8 (-20.32)	-0.325 (-8.26)	-0.525 (-13.34)	80 (2032)	-0.275 (-6.98)	-0.1 (-2.54)	-0.45 (-11.43)
34 (864)	-0.9 (-22.86)	-0.4 (-10.16)	-0.6 (-15.24)	82 (2083)	-0.25 (-6.35)	-0.1 (-2.54)	-0.4 (-10.16)
36 (914)	-0.975 (-24.77)	-0.425 (-10.80)	-0.675 (-17.14)	84 (2134)	-0.225 (-5.72)	-0.1 (-2.54)	-0.325 (-8.26)
38 (965)	-1 (-25.4)	-0.5 (-12.70)	-0.725 (-18.42)	86 (2184)	-0.165 (-4.19)	-0.075 (-1.90)	-0.275 (-6.98)
40 (1016)	-1 (-25.4)	-0.5 (-12.70)	-0.75 (-19.05)	88 (2235)	-0.2 (-5.08)	-0.05 (-1.27)	-0.25 (-6.35)
42 (1067)	-1.025 (-26.04)	-0.5 (-12.70)	-0.775 (-19.68)	90 (2286)	-0.15 (-3.81)	-0.05 (-1.27)	-0.225 (-5.72)
44 (1118)	-1.05 (-26.67)	-0.475 (-12.06)	-0.825 (-20.96)	92 (2337)	-0.15 (-3.81)	0	-0.225 (-5.72)
46 (1168)	-1.075 (-27.30)	-0.5 (-12.70)	-0.85 (-21.59)	94 (2388)	-0.115 (-2.92)	0	-0.175 (-4.44)
				96 (2438)	-0.1 (-2.54)	0	-0.175 (-4.44)

Table 19
Average rut depth measured for lane 2-1
with powdered rubber wearing course

DATE	PASS NO.	Cumulative 18-kip (80 kN) ESALs	AVG RUT, in(mm)
2/2/99	0	0	0.00 (0.00)
3/18/99	25000	34425	0.12 (3.05)
3/29/99	50000	68850	0.17 (4.32)
4/8/99	75000	103275	0.18 (4.57)
4/22/99	100000	137700	0.19 (4.83)
5/17/99	150000	206550	0.27 (6.86)
5/27/99	175000	240975	0.29 (7.37)
6/10/99	200000	275400	0.30 (7.62)
6/22/99	225000	309825	0.33 (8.38)
7/20/99	275000	378675	0.36 (9.14)
8/9/99	300000	413100	0.37 (9.40)
8/23/99	325000	447525	0.40 (10.16)
9/8/99	350000	481950	0.41 (10.41)
9/22/99	375000	516375	0.41 (10.41)
10/4/99	400000	550800	0.41 (10.41)
10/21/99	425000	631050	0.41 (10.41)
12/6/99	500000	871800	0.41 (10.41)
12/20/99	525000	952050	0.43 (10.92)
1/11/00	550000	1194800	0.44 (11.18)
2/7/00	600000	1517800	0.44 (11.18)
5/1/00	675000	2133650	0.44 (11.18)
10/9/00	750000	3012200	0.56 (14.22)
11/27/00	800000	3994700	0.56 (14.22)

Table 20
Average rut depth measured for lane 2-2
with powdered rubber base course

DATE	PASS NO.	Cumulative 18-kip (80 kN) ESALs	AVG RUT, in(mm)
2/2/99	0	0	0.00 (0.00)
3/18/99	25000	34425	0.04 (1.02)
3/29/99	50000	68850	0.10 (2.54)
4/8/99	75000	103275	0.10 (2.54)
4/22/99	100000	137700	0.10 (2.54)
5/17/99	150000	206550	0.13 (3.30)
5/27/99	175000	240975	0.14 (3.56)
6/10/99	200000	275400	0.18 (4.57)
6/22/99	225000	309825	0.19 (4.83)
7/20/99	275000	378675	0.22 (5.59)
8/9/99	300000	413100	0.22 (5.59)
8/23/99	325000	447525	0.24 (6.10)
9/8/99	350000	481950	0.25 (6.35)
9/22/99	375000	516375	0.26 (6.60)
10/4/99	400000	550800	0.26 (6.60)
10/21/99	425000	631050	0.26 (6.60)
12/6/99	500000	871800	0.26 (6.60)
12/20/99	525000	952050	0.26 (6.60)
1/11/00	550000	1194800	0.26 (6.60)
2/7/00	600000	1517800	0.26 (6.60)
5/1/00	675000	2133650	0.26 (6.60)
10/9/00	750000	3012200	0.36 (9.14)
11/27/00	800000	3994700	0.36 (9.14)
12/31/00	850000	4977200	0.36 (9.14)

Table 21
Average rut depth measured for lane 2-3 with conventional HMA

DATE	PASS NO.	Cumulative 18-kip (80 kN) ESALs	AVG RUT, in(mm)
2/2/99	0	0	0.00 (0.00)
3/18/99	25000	34425	0.03 (0.76)
3/29/99	50000	68850	0.07 1.78)
4/8/99	75000	103275	0.10 (2.54)
4/22/99	100000	137700	0.12 (3.05)
5/17/99	150000	206550	0.19 (4.83)
5/27/99	175000	240975	0.22 (5.59)
6/10/99	200000	275400	0.23 (5.84)
6/22/99	225000	309825	0.27 (6.86)
7/20/99	275000	378675	0.32 (8.13)
8/2/99	300000	413100	0.35 (8.89)
8/23/99	325000	447525	0.35 (8.89)
9/8/99	350000	481950	0.38 (9.65)
9/22/99	375000	516375	0.39 (9.91)
10/4/99	400000	550800	0.39 (9.91)
10/20/99	425000	631050	0.39 (9.91)
12/20/99	525000	952050	0.39 (9.91)
1/11/00	550000	1194800	0.39 (9.91)
2/7/00	600000	1517800	0.40 (10.16)
5/1/00	675000	2133650	0.40 (10.16)
10/9/00	750000	3012200	0.55 (13.97)
11/27/00	800000	3994700	0.55 (13.97)

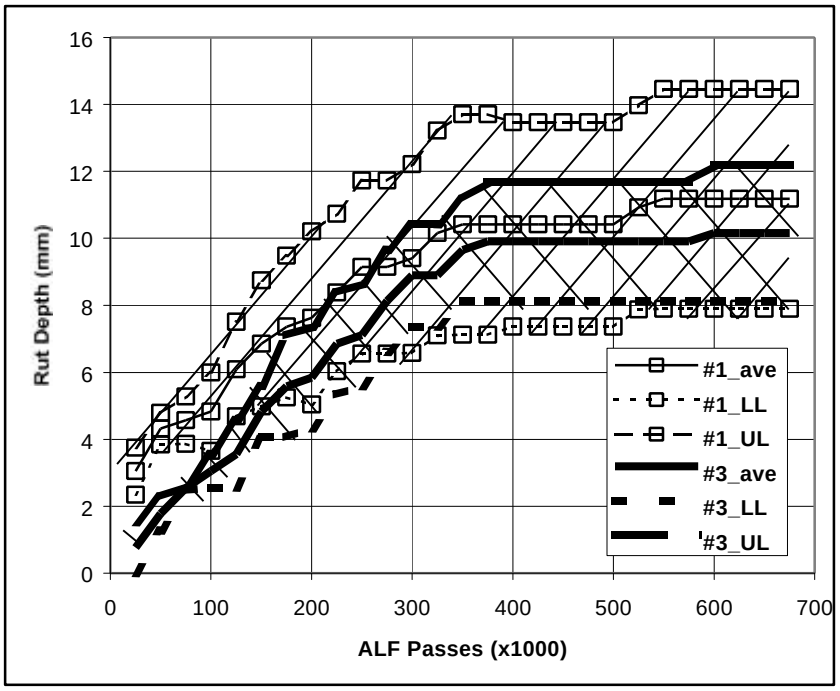

Figure 19
Rut depth versus ALF passes for lanes 2-1 and 2-3

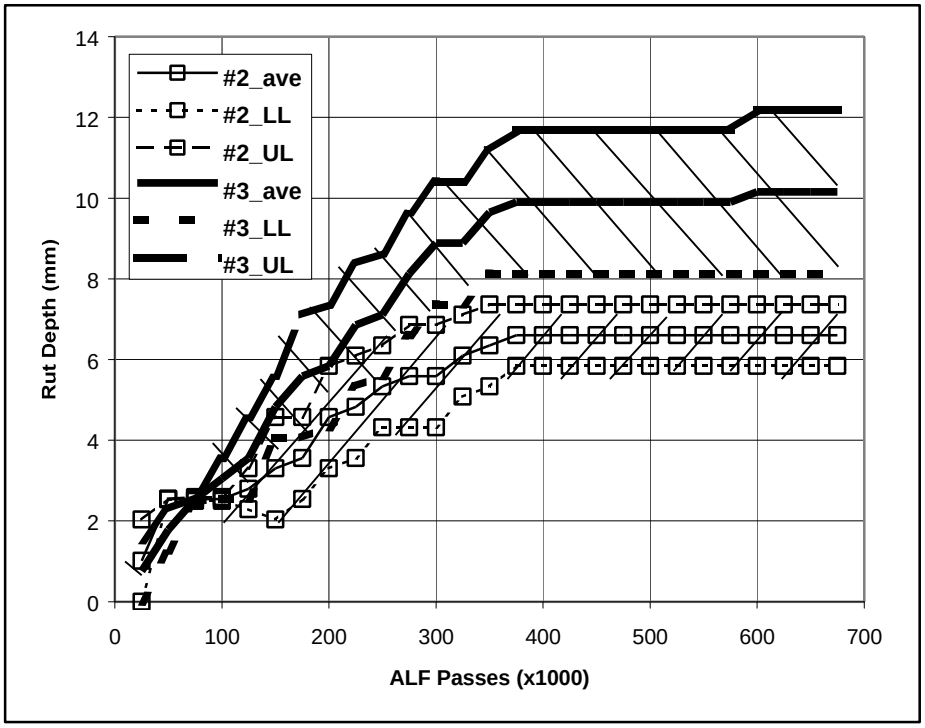

Figure 20
Rut depth versus ALF passes for lanes 2-2 and 2-3

Numerical Simulation of Pavement Test Lane Behavior

As mentioned in the methodology section, simulations of pavement behavior were performed using both ABAQUS 3-D and FLEXPASS finite element computer programs. The ABAQUS predictions were made for primary response of the pavement to ALF loading using 3-D viscoplastic material characterization. The primary responses were stress, strain, and deflection due to imposed ALF loading. The FLEXPASS predictions included rutting, cracking, and serviceability using the models initially included in VESYS and imported into FLEXPASS.

ABAQUS Numerical Simulation Results

Figure 21 presents the calculated shear strains and longitudinal strains at the bottom of the combined wearing and binder courses (depth = 88.9 mm) and at the bottom of the asphalt base course (depth = 176.8 mm) for the test lanes. The designations of direction were as follows: 1 – transverse direction; 2 – the longitudinal (traffic) direction, and; 3 – the vertical (depth) direction. Hence, the symbol "E23" means the shear strain along a plane defined by the longitudinal and vertical directions. It appeared that lane 2-2 had smaller longitudinal and shear strains than the control lane (lane 2-3) at the bottom of the wearing course. Fewer shear strains at the surface layer reduce the susceptibility of surface-generated rutting. Lower longitudinal tensile strains reduce the susceptibility of the pavement to fatigue cracking. The shear strains of all three lanes at the bottom of the asphalt base course were similar. Their magnitudes were significantly reduced when compared to those in the wearing course.

There were no significant differences in the shear and longitudinal tensile strains between lane 2-1 (with PRM-HMA surface wearing course) and lane 2-3 (control lane with conventional asphalt mixtures).

Figure 22 presents the results of calculated total dynamic surface deflections of the three lanes across the wheel path in the transverse direction. In these calculations, the material properties are described as time-dependent functions. It appeared that lane 2-2 had the smallest maximum deflection, followed by lanes 2-1 and 2-3, respectively. The differences of surface deflections between lanes 2-1 and 2-3 were not as significant as those between lane 2-2 and lanes 2-1 and 2-3. This result matched the observations from the Dynaflect and FWD tests.

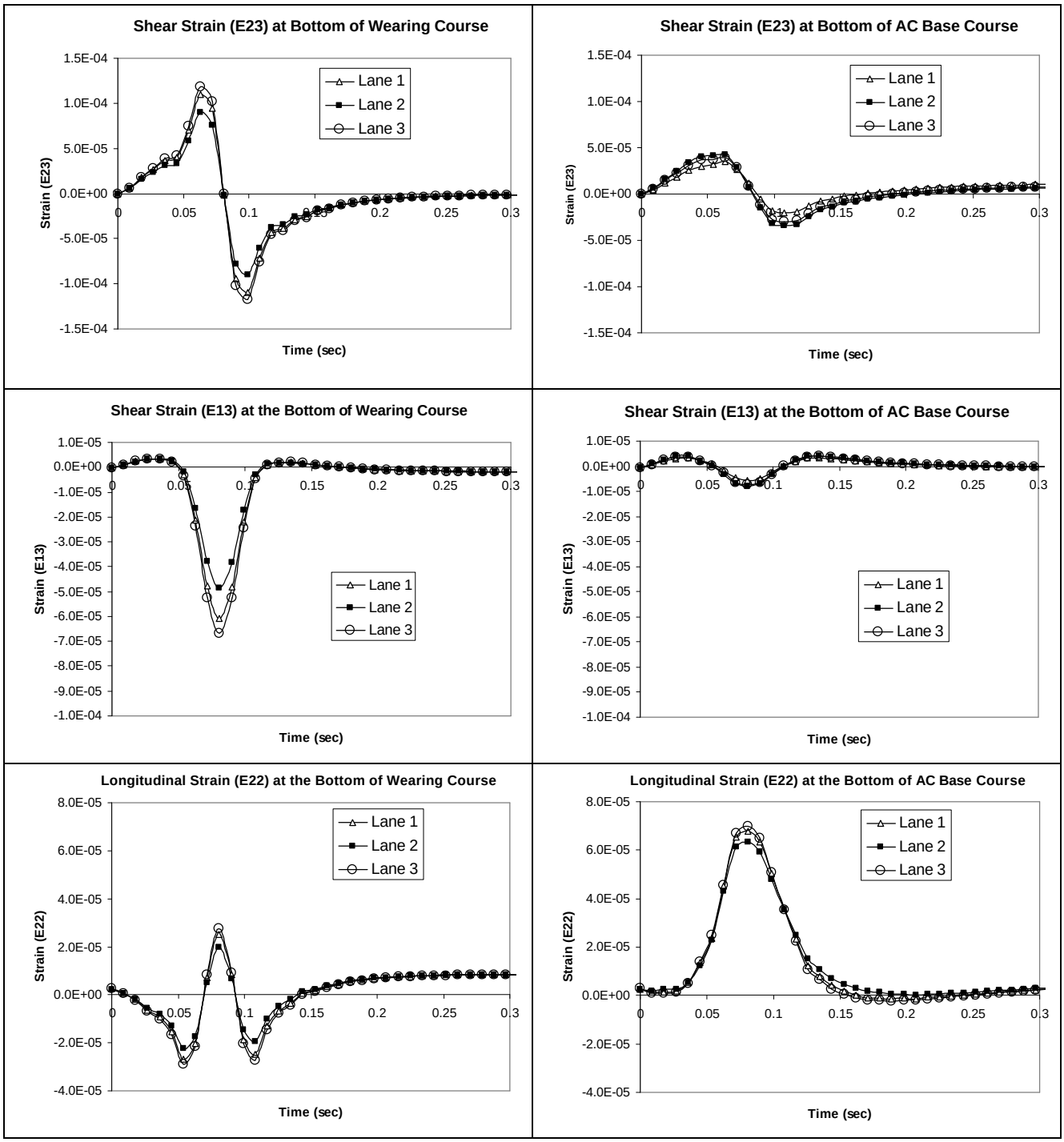

Figure 21
ABAQUS-predicted pavement dynamic strain response under ALF loading
[35]

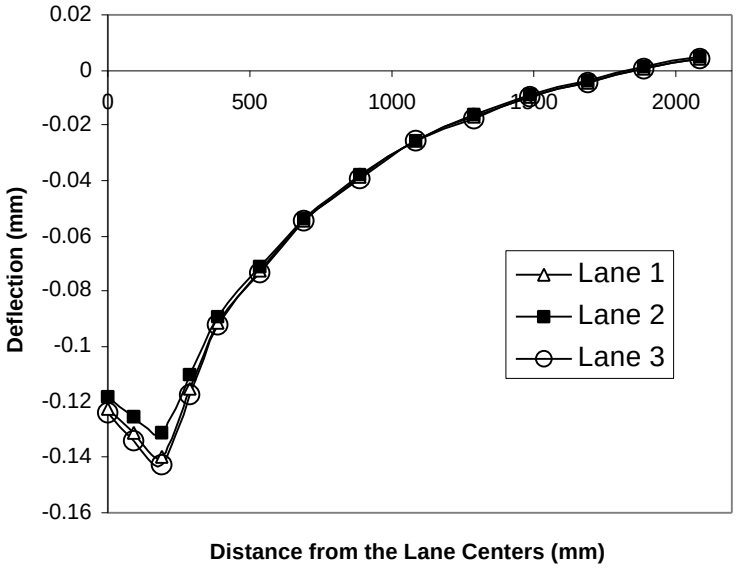

Figure 22
ABAQUS-calculated maximum surface deflections under the ALF load

The 3-D viscoplastic analysis demonstrated the effect of the viscosity characteristics on the response of the HMA; the strain lagged behind the instantaneous elastic response. Figure 23 presents a typical dynamic response of longitudinal strain at the bottom of the base course. In comparing this measured response to the corresponding computed dynamic response from the 3-D finite element analysis, a very close response pattern was observed for all lanes. The measured longitudinal strains at the bottom of the binder and base courses were around $1.5x10^{-5}$ and $4.5x10^{-5}$ for the lane 2-2, while the 3-D FEM predicted $2.0x10^{-5}$ and $6.2x10^{-5}$, respectively. The differences between measured and calculated strains could be explained as either measurement errors or as a result of the selection of material parameters used in the 3-D FEM analysis. Despite these differences, the 3-D FEM produced the same ranking among the lanes as did the field strain measurements.

FLEXPASS Performance Predictions

Figure 24 shows the FLEXPASS rutting predictions using the as-constructed cross sections for all three lanes as shown in Figure 25. The predicted rut depths for lanes 2-1 and 2-3 are similar. These results are consistent with the field observations and also with the laboratory material characterization, which showed that the properties of the wearing

course with or without powdered rubber were similar *[40]*. Lanes 2-1 and 2-3 showed no difference in the rut depth development up to

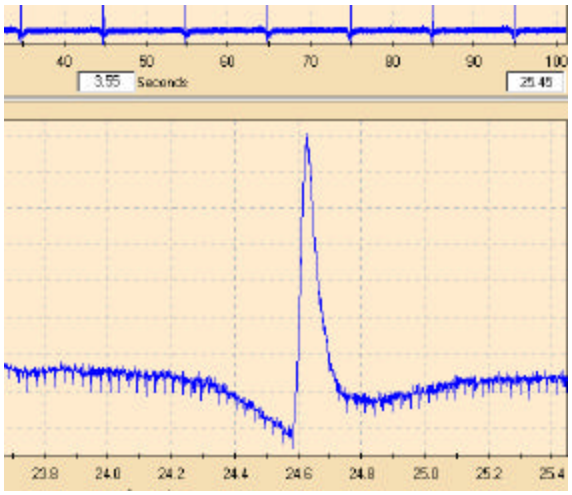

Figure 23
A typical measured longitudinal strain response curve at the bottom of the base

500,000 ESALs. This initial linear rutting component is due to densification of the HMA under traffic and is typical behavior for HMA pavements in the field. After this initial densification, the rut depth development rate slowed down for all three lanes for the load interval between 500,000 and 1,500,000 ESALs. The slope of the rut depth development line became even smaller after 1.5 million ESALs until the end of loading.

This flattening out of the slope of the rut development line is also typical of in-service pavements. Typical HMA pavements densify under traffic during the first two to three years of service and then the rut depth slope will remain low until either a base failure occurs or until the mix becomes plastic. After initial densification, if the voids in the HMA are between 3 to 6 percent, the mix probably will not exhibit plastic behavior.

The final predicted rut depth for lane 2-1 was 0.67 inch (17.02 mm), for lane 2-2 was 0.31 inch (7.87 mm), and for lane 2-3 was 0.64 inch (16.26 mm). The trends for these observations are consistent with the ALF field data while the FLEXPASS predictions were about 20 percent higher than the field values for lane 2-1 and 2-3 and about 15 percent lower than the field value for lane 2-2.

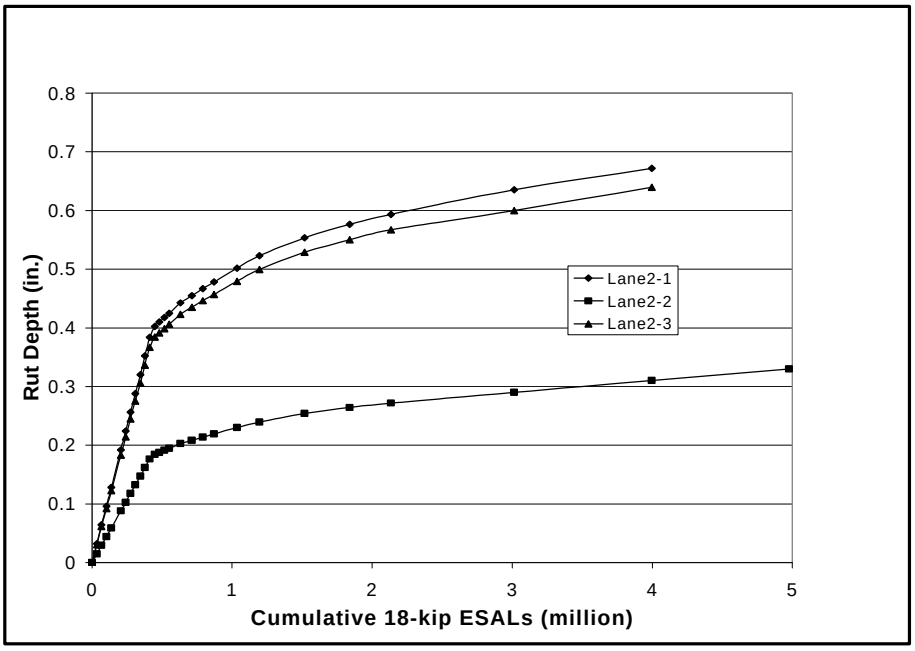

Figure 24
Comparison of predicted rut depth for all ALF test lanes

Lane 2-1 PRM Wearing Course	Lane 2-2 PRM Base Course	Lane 2-3 Control
4.2" Type 8F Wet Rouse Wearing & Binder Courses	4.6" Type 8F Wearing & Binder Courses	4.0" Type 8F Wearing & Binder Courses
2.6" Base Course	3.3" Wet Rouse Base Course	3.2" Base Course
8.5" Crushed Stone Base	8.5" Crushed Stone Base	8.5" Crushed Stone Base
10.0" Soil Cement Subbase	10.0" Soil Cement Subbase	10.0" Soil Cement Subbase
Embankment	Embankment	Embankment

Figure 25
Layer thickness of test lanes as determined from elevations taken during construction

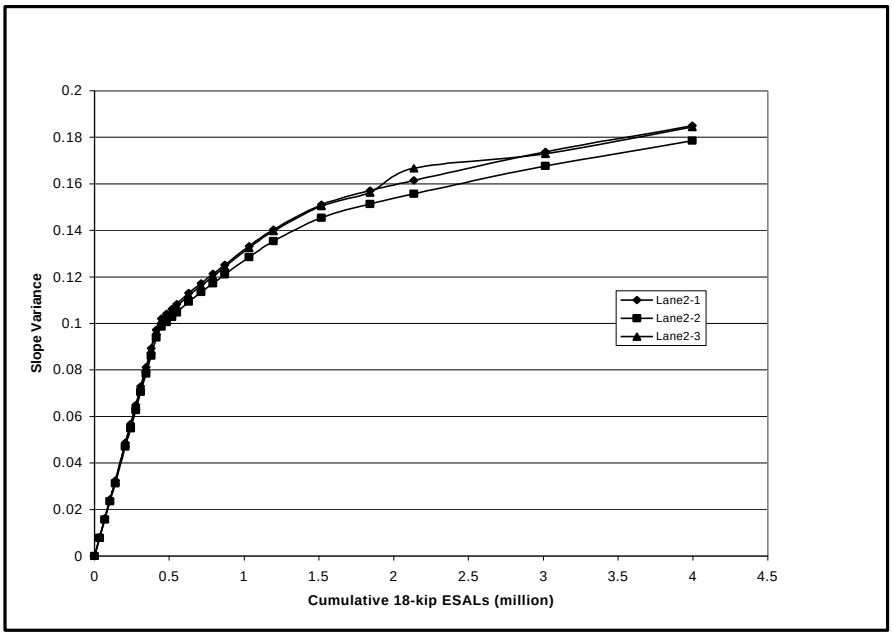

Figure 26
FLEXPASS-predicted slope variance for all ALF test lanes

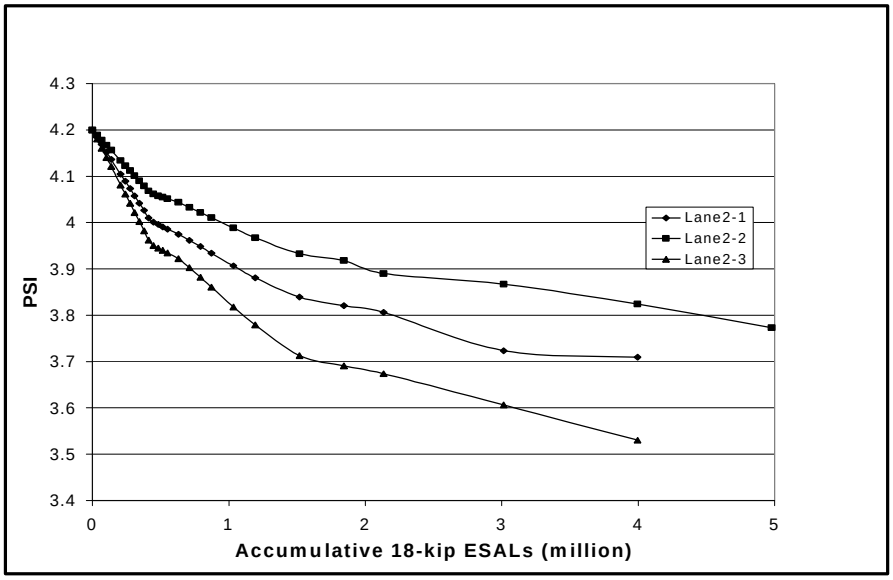

Figure 27
FLEXPASS-predicted PSI for all ALF test lanes

Figure 26 shows the FLEXPASS predicted slope variance for all the test lanes. The predicted slope variance developed at a rapid rate before 500,000 ESALs for all three lanes; then the development slowed down for the balance of the loading. The slope variance of lane 2-2 was the lowest, but the other two lanes showed similar slope variance development curves.

FLEXPASS did not predict any fatigue cracking development for any of the test lanes, a result consistent with the field observations.

Figure 27 shows the predicted PSI for all three test lanes. The initial PSI was assumed to be 4.2. The comparison showed that the PSI of lane 2-3 decreased faster than the other two lanes. Since the ALF loading was terminated when the average rut depth reached 0.5 inches (12.7 mm), the PSI did not reach the terminal value. Under normal service conditions, traffic would continue to load the pavement until either the PSI reached a terminal value or until the rut depth produced hazardous driving conditions.

Comparison between Predicted and Observed Rutting

Because the only observed distress was rutting, only the comparison between predicted and observed rutting will be made. Figure 28 shows the predicted rutting development from FLEXPASS and the measured rutting for lane 2-1. Field rutting began at 34,425 ESALs and increased rapidly to around 0.40 inch (10.16 mm) at about 500,000 ESALs. The rut depth remained relatively constant until approximately 2 million ESALs. After 2 million ESALs, the rut depth began to increase sharply as the half axle load increased above 14.35 kips (63.71 kN). The observed performance of lane 2-1 shows two of the three typical phases of rutting that are observed in HMA pavements. In phase I, the initial rutting increases at a rapid rate early in the life of the pavement, which in Figure 28 is from zero to about 500,000 ESALs. Phase II is the stable region of performance where the slope of the rutting curve is fairly flat. The length of phase II varies and in Figure 28 lasts from about 500,000 ESALs until about 2,200,000 ESALs corresponding to wheel loads increasing from 9,750 to 14,350 lbs (43.29 to 63.71 kN) on the half single axle. Figure 28 shows a rapid increase in rutting starting at about 2,200,000 ESALs and continuing as the wheel load increases from 14,350 to 16,650 lbs (63.71 to 73.93 kN) at 3 million ESALs. This trend continued as the wheel load increased to 18,950 lbs (84.14 kN) until testing was terminated at 4 million ESALs for lane 2-1. It should be noted that while the rate of rutting increased as the wheel loads increased from 14,350 to 18,950 lbs (63.71 to 84.14 kN), there was little evidence of shear flow adjacent to the wheel loaded

area. As a result of this observation, the authors believe that section 2-1 pavements were still behaving in the phase II region of rutting and that the rutting was a result of additional densification of the HMA under the heavier loads. The FLEXPASS prediction also showed that rutting increased rather rapidly at the early loading stage until at about 450,000 ESALs, where the rate of rutting development decreased. The predicted rut depth was about 20 percent greater than the measured field data. The pattern of predicted behavior from FLEXPASS is typical of that obtained from computer programs which include material

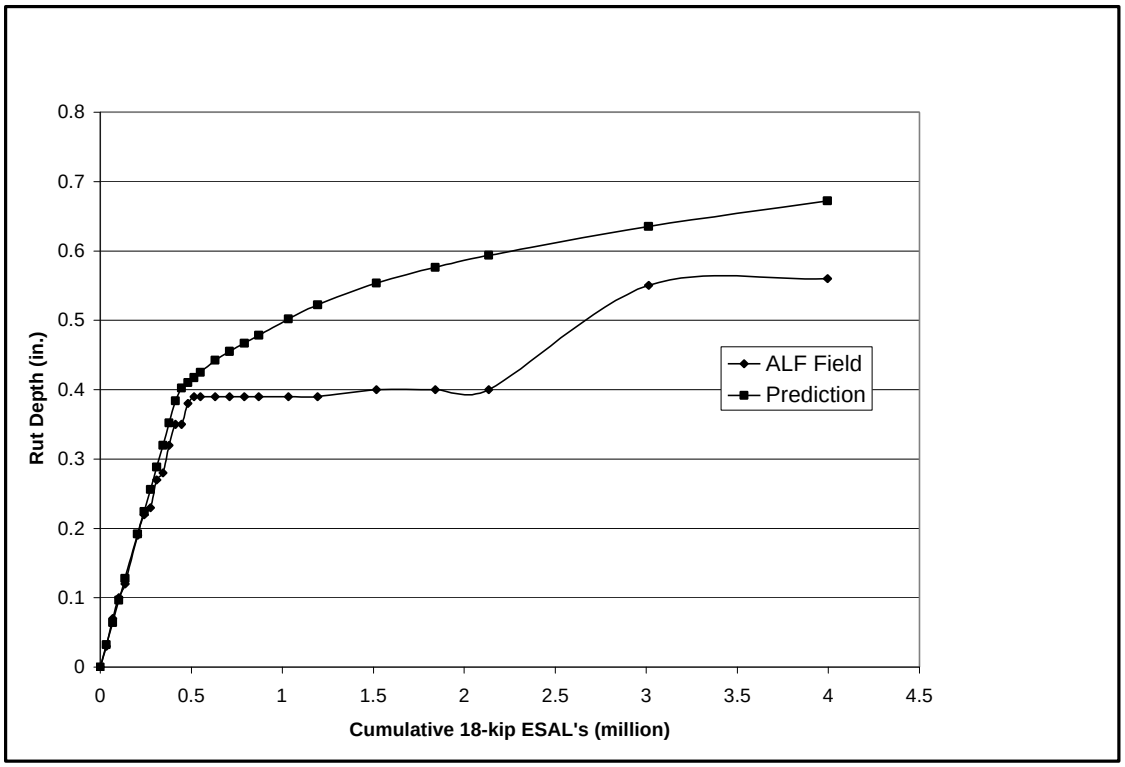

Figure 28
Comparison between field measured and predicted rutting for lane 2-1 with PRM wearing course

characterizations using creep tests to model the behavior of materials in phases I and II of rutting. The traffic in FLEXPASS is characterized by ESALs and not individual axle loads, so the effect of increasing the axle load is accomplished by increasing the rate of ESALs per traffic period. Because the increased axle loads are applied when the rate of rutting is nearly flat, the influence of these heavier axle loads is lower in the predictions than is shown in the field data.

Figure 29 show the comparison of rutting development for FLEXPASS prediction and field measurements for test lane 2-2, which includes the PRM base. The field results showed that rutting began at 34,425 ESALs and increased rapidly to around 0.26 inch (6.60 mm) at about 500,000 ESALs. It should be noted again that this level of rutting is typical of many pavements which experience 0.25 to 0.30 in. (6.35 to 7.62 mm) of rutting in the first two to three years of service. In lane 2-2, the rutting remained constant until about 2,100,000 ESALs where the load had increased to 14,350 lbs (63.71 kN). After that, the rut depth increased rapidly. The FLEXPASS prediction also showed that rutting increased rather quickly at the early loading stage until 0.20 in. (5.08 mm) at about 550,000 ESALs. Then the rate of rutting development began decreasing. The FLEXPASS prediction is lower than the field result, but as the axle loads increased, the predicted and observed rut depths were very similar.

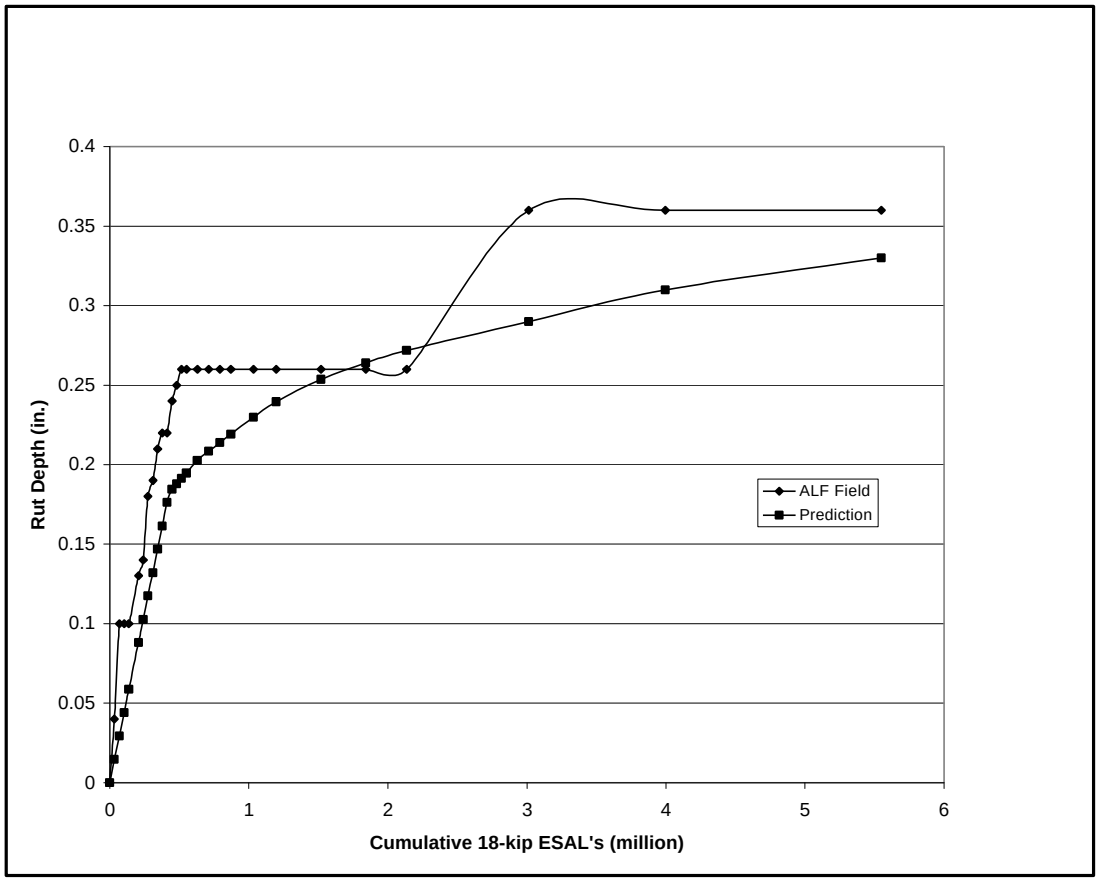

Figure 29
Comparison between field measured and predicted rutting for lane2-2 with PRM base

Figure 30 shows the comparison of rutting development for FLEXPASS prediction and field measurement of ALF test lane 2-3, the conventional HMA control section. The field results showed that rutting began at very early loading level and increased rapidly to around 0.41 in. (10.41 mm) at about 450,000 ESALs. The rut pattern for the conventional materials showed a rapid rise in rutting with each increase in axle load, but then rutting leveled off. The FLEXPASS prediction also showed that rutting increased more steeply at the early loading stage until 0.40 in. (10.16 mm) at about 550,000 ESALs. Then the rate of rutting development slowed down, but rutting developed gradually as the wheel loads increased because the number of ESALs per axle pass increased as the loads increased. The predicted rutting was less than the field rutting until around 500,000 ESALs. After that loading level, the predicted rutting exceeded the observed rutting. The predicted rut depth was about 15 percent larger than the observed field rutting when testing terminated.

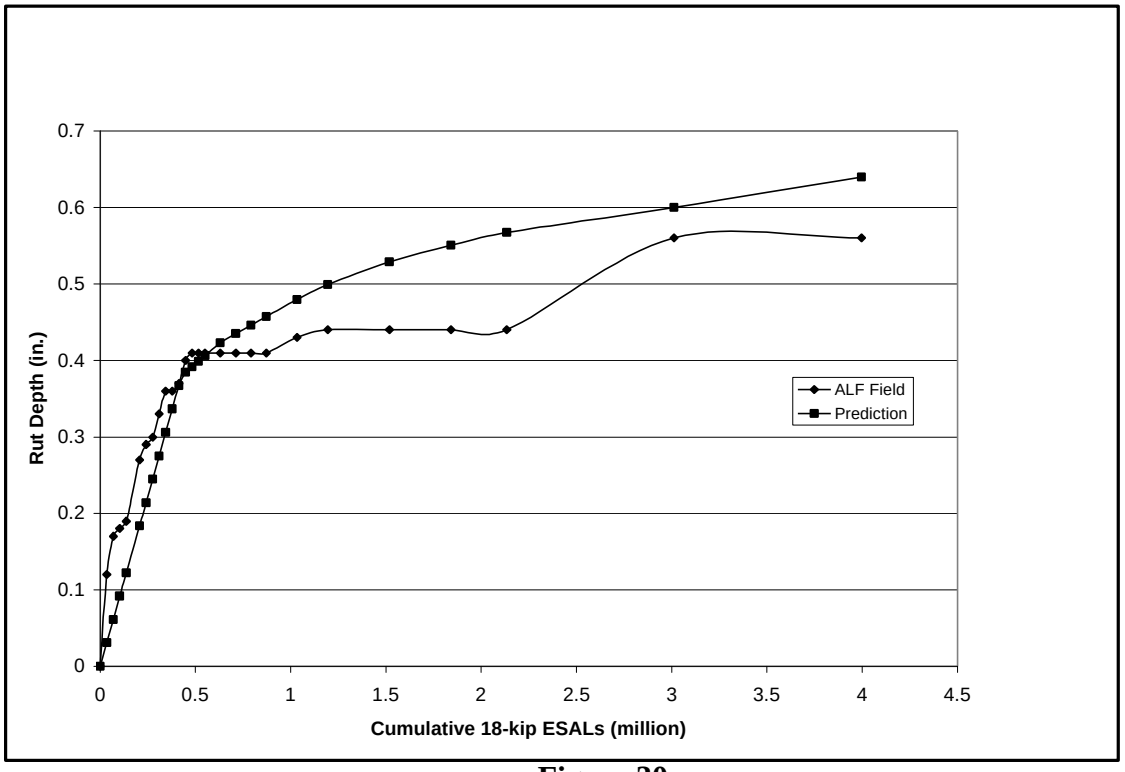

Figure 30
Comparison between field measured and predicted rutting for lane 2-3 ,control lane, with conventional materials

Calculations to Determine SN

As described in the methodology section, three techniques were used to calculate structural numbers for the ALF test lanes.

SN Calculated from AASHTO Flexible Pavement Design Equation

The SN calculations from the AASHTO flexible pavement design equation were performed using the predictions of serviceability at the end of testing using FLEXPASS. Additionally, the resilient modulus values for the subgrade soil were determined from laboratory testing conducted at the LTRC laboratories. A relationship between resilient modulus and deviator stress was developed for three confining pressures of 0.2, 3.0, and 6.0 psi (1.38, 20.7, and 41.4 kPa)[*41*]. For a confining pressure of 2.0 psi (13.8 kPa), and deviator stresses of 2.0 psi (13.8 kPa) and 3.0 psi (20.7 kPa), resilient moduli for the subgrade soil were determined to be 4,100 psi (28.3 MPa) and 3,600 psi (24.8 MPa), respectively. SN values were calculated for each of these subgrade moduli using the following data from the ALF test lanes:

z_R = -1.645 for R = 95 percent

s_o = 0.47, for Louisiana conditions

W_{18} = 3,995,600 ESALs

In addition to the data noted above, the FLEXPASS predicted serviceability at the end of traffic for each of the test lanes, table 22, was used in the calculations.

SN Calculated from Deflection Data

Structural number (SN) was calculated from deflection data using the techniques described in the methodology section of this report. The SNs generated using these techniques are shown in table 23 and plotted in figures 31 and 32, presenting the SN data calculated from falling weight deflectometer (FWD) and Dynaflect deflections,

respectively. The curves shown on these figures were drawn to demonstrate the general trends in the data. The curves were drawn free style and do not represent any type of statistical curve. Generally the data show that SN varies primarily with the season of the year and the primary effect appears to be temperature of

Table 22
Calculations of SN using AASHTO flexible pavement design equation

Lane No.	Serviceability Level		Calculated SN		
	Initial	FLEXPASS predicted Terminal	Subgrade Modulus, psi (MPa)		Average
			3,600 (24.8)	4,100 (28.3)	
2-1,PRM Wearing	4.2	3.7093	8.62	8.30	8.46
2-2,PRM Base	4.2	3.8245	9.35	9.01	9.18
2-3,Conventional	4.2	3.5303	7.83	7.53	7.68

the pavement section. Pavement temperature is greatest during the summer months and lowest during the winter. The data in table 23 shows that summertime temperatures occur when the ALF load was between 150,000 and 350,000 applications and between 675,000 and 700,000 applications. In figures 31 and 32, the SN-values are lowest during these two high temperature periods. SN-values were highest during February-March 1999 (0 to 50,000 ALF load applications) and during December – March 2000 (500,000 to 600,000 ALF load applications). During the other times, the SN-values were transitioning between low and high temperature periods. SN-values calculated from both FWD and Dynaflect deflections show the same trends in figures 31 and 32. It should also be noted that the temperature effects are so large that they overwhelm other expected trends in the data, such as expecting the SN-values to decrease as the distress and ALF load applications increase.

Since the SN-values in figures 31 and 32 cycle produce an average effect, the SN data from appropriate columns in table 23 was averaged as shown in the last row of the table. In order to evaluate these calculated values of SN, one must compare them to the SN values generated using the structural coefficient, a-value, and the thickness of each layer

in each of the test lanes. Calculation of SN_i for each layer is shown in table 24. In the cases where the a-value is unknown, i.e., for the PRM wearing and base courses in lanes

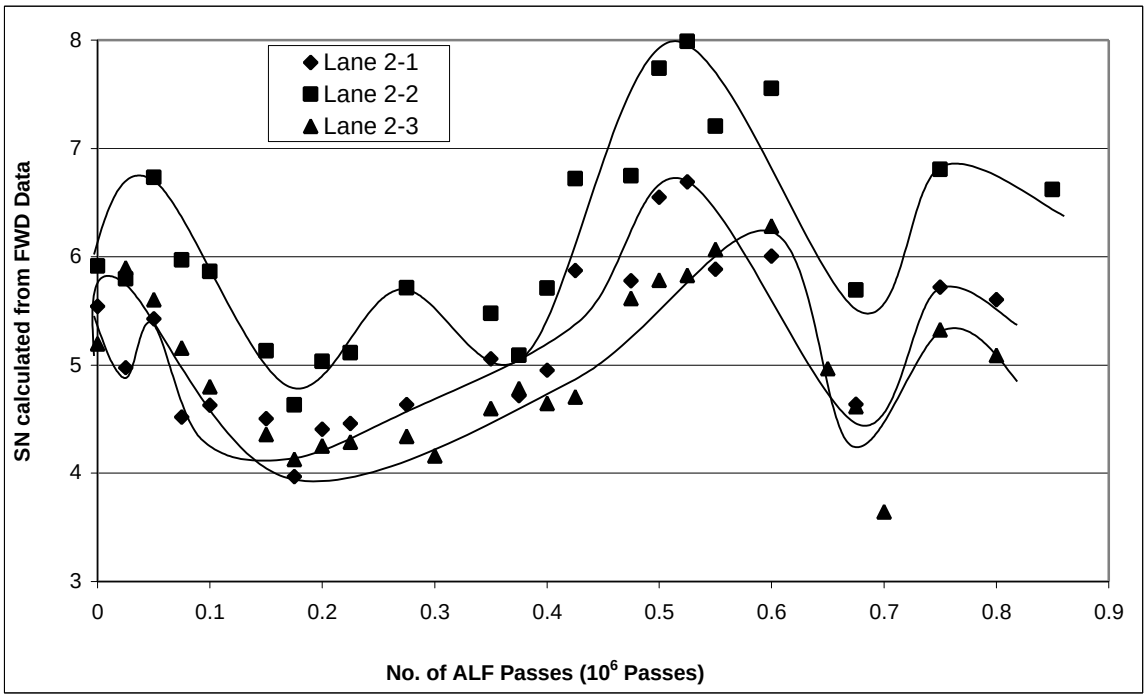

Figure 31
Variation in SN, calculated from FWD data, during ALF testing

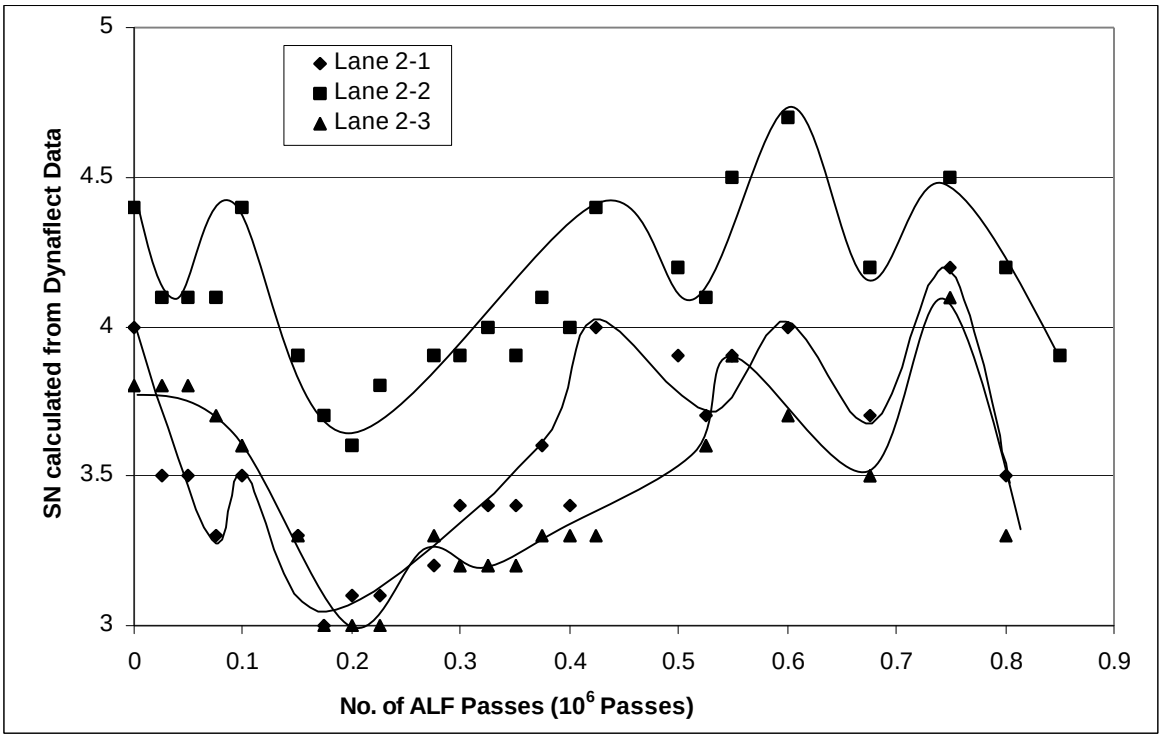

Figure 32
Variation in SN, calculated from Dynaflect data, during ALF testing

2-1 and 2-2, an unknown is included in table 24. Notice that only lane 2-3 has a known SN for the whole pavement cross section and this known value provided guidance in selecting from among the three methods used to calculate SN for the actual test lanes at the ALF site. In the calculations for SN for lane 2-3, the layer thickness is from the construction data and the a-values are from the various engineering directives developed by the DOTD. The a-value selected for the PRM base was 0.40 since this base is a binder course aggregate gradation with an AC-30 asphalt and a previous engineering directive prescribed an a-value of 0.4 for this material. In order to compare the SNs generated using the three methods, the averages from all sets of calculations are summarized in table 25.

Remembering that SN_{2-3} is 5.63 (table 24), it is immediately obvious that the SN_{2-3} calculated using the FWD data (table 23) are closer to 5.63 than the values from the Dynaflect or those back calculated from the AASHTO equation. In fact, the Dynaflect

SNs are too low to be reasonable while the back calculated AASHTO values are too high to be reasonable. Based on these results, the authors have elected to calculate the structural coefficients for the PRM wearing course and PRM base using the SN values calculated from the FWD data.

Lane 2-3 is used to normalize the FWD-calculated SNs to the values used in Louisiana for flexible pavement design. This normalization process occurs by taking the difference between the FWD calculated SN and the SN_{design} value of 5.63 (5.64 – 5.63 = 0.10) and subtracting that value from the SN for lanes 2-1 and 2-2 in table 25 under the Falling Weight Deflectometer column. This calculation gives a normalized $SN_{2\text{-}1}$ of 5.20 and $SN_{2\text{-}2}$ of 6.14. Now, the a-value for the powdered rubber wearing course can be calculated by setting the equation in the Total SN row for Lane 2-1 of table 24 equal to 5.20. Solving for a_{PRMW} yields 0.25 as the structural coefficient for the powdered rubber wearing course. Setting the equation in the Total SN row for Lane 2-2 of table 24 equal to 6.14 yields an a_{PRMB} for the powdered rubber base of 0.45.

These data indicate that the addition of powdered rubber in the wearing course produces a material that with slightly poorer performance than that of the normal Type 8 materials currently being constructed by the LaDOTD. However, the addition of powdered rubber

Table 23
Calculations of SN using Dynaflect and FWD deflection data

Load, lb.	No. of ALF Passes	Date data was collected	AASHTO Structural Number, SN					
			SN Calculated from FWD Data			SN Calculated from Dynaflect Data		
			Lane 2-1, PRM Wearing Course	Lane 2-2, PRM Base Course	Lane 2-3, Control, Convent. HMA	Lane 2-1, PRM Wearing Course	Lane 2-2, PRM Base Course	Lane 2-3, Control, Convent. HMA
9750	0	2/01/99	5.542	5.915	5.197	4.0	4.4	3.8
	25000	3/18	4.976	5.797	5.898	3.5	4.1	3.8
	50000	3/29	5.427	6.734	5.604	3.5	4.1	3.8
	75000	4/08	4.517	5.971	5.160	3.3	4.1	3.7
	100000	4/22	4.626	5.864	4.799	3.5	4.4	3.6
	150000	5/17	4.504	5.132	4.359	3.3	3.9	3.3
	175000	5/27	3.970	4.630	4.129	3.0	3.7	3.0
	200000	6/10	4.406	5.034	4.251	3.1	3.6	3.0
	225000	6/22	4.459	5.115	4.287	3.1	3.8	3.0
	275000	7/20	4.634	5.713	4.341	3.2	3.9	3.3
	300000	8/02			4.160	3.4	3.9	3.2
	325000	8/23				3.4	4.0	3.2
	350000	9/08	5.059	5.479	4.597	3.4	3.9	3.2
	375000	9/22	4.715	5.091	4.782	3.6	4.1	3.3
12050	400000	10/04	4.951	5.710	4.646	3.4	4.0	3.3
	425000	10/21	5.873	6.722	4.705	4.0	4.4	3.3
	475000	11/18	5.778	6.747	5.617			
14350	500000	12/10	6.549	7.741	5.786	3.9	4.2	
	525000	12/20/99	6.693	7.989	5.830	3.7	4.1	3.6
	550000	1/11/00	5.884	7.206	6.068	3.9	4.5	3.9
	600000	2/07	6.007	7.554	6.283	4.0	4.7	3.7
16650	650000	3/02			4.966			
	675000	5/01	4.637	5.692	4.616	3.7	4.2	3.5
	700000	5/31			3.644			
18950	750000	10/09	5.719	6.806	5.327	4.2	4.5	4.1
21250	800000	11/27/00					4.2	
	800000	3/13/01	5.604		5.090	3.5		3.3
	850000	3/13/01		6.622			3.9	
Average SN			5.206	6.148	5.636	3.56	4.11	3.45

Table 24
Components of SN for the three test lanes

Layer	Lane 2-1, PRM Wearing			Lane 2-2, PRM Base			Lane 2-3, Control		
	Thick-ness	**a-value**	**SN_{2-1}**	**Thick-ness**	**a-value**	**SN_{2-2}**	**Thick-ness**	**a-value**	**SN_{2-3}**
Wearing Cr.	1.5	a_{PRMW}	1.5* a_{PRMW}	1.5	0.44	0.66	1.5	0.44	0.66
Binder Course	2.7	0.44	1.19	3.1	0.44	1.36	2.5	0.44	1.10
Base	2.6	0.40	1.04	3.3	a_{PRMB}	3.3* a_{PRMB}	3.2	0.40	1.28
Cr. Stone	8.5	0.14	1.19	8.5	0.14	1.19	8.5	0.14	1.19
Soil Cem.	10.0	0.14	1.40	10.0	0.14	1.40	10.0	0.14	1.40
Total SN			4.82+ 1.5* a_{PRMW}	Total SN		4.61 + 3.3* a_{PRMB}	Total SN		5.63

Table 25
Average calculated structural number (SN)

Lane No.	AASHTO	Dynaflect	Falling Weight Deflectometer
2-1, PRM Wearing	8.46	3.56	5.21
2-2, PRM Base	9.18	4.11	6.15
2-3, Control	7.68	3.45	5.64

at a rate of 10 percent by weight of the asphalt into the base course improves its structural coefficient from 0.40 to 0.45, an improvement of 12.5 percent. Since the addition of the powdered rubber only increases the cost of the AC-30 about 10 percent, its addition to the base appears to be cost effective. In fact, the addition of the powdered rubber to the AC-30 produces a material that is very similar to the current PAC-40 materials, see the discussion of test results from table 2. One may conclude that these results suggest that the LaDOTD include powdered rubber or polymers in any hot mix asphalt layers below the binder course.

CONCLUSIONS

The purpose of this project was to test, evaluate, and compare the performance of HMA and powdered rubber HMA materials used in the construction of three test lanes at the PRF. With the results from the ALF testing, the relative strength coefficient and a-value used in pavement design were determined for each of the asphalt rubber materials. Each material's cost effectiveness and optimal location in the pavement were also assessed. Numerical simulations of the test lanes were also generated to determine if computer models could be used to extend the application of the field studies. We compared the distress and other field observations from test lanes loaded with the ALF to distresses and responses of the test lanes which were predicted in the numerical simulations. Based on the discussion in this report, the following conclusions are presented:

1. FLEXPASS can be used to successfully model Louisiana flexible pavements. All three of the test lanes exhibited agreement between FLEXPASS-predicted rutting and observed field.

2. ABAQUS can be used to calculate the primary responses and deflections from not only ALF loads but also the loads applied by both the Dynaflect and Falling Weight Deflectometer. Since the run times for ABAQUS are still quite large, it does not appear to be a practical program for analyzing loading situations where a very large number of loads are applied. However, ABAQUS is a very powerful program that can be used to analyze materials with very complicated material characteristics and it should continue to be used as a research tool.

3. Powdered rubber, or polymers, should be added to AC-30 to form the binders used in asphalt bases. The resulting structural coefficient, a-value, for the powdered rubber base is 0.45 compared to 0.40 for a base of binder course

gradation mixed with AC-30. Addition of the powdered rubber increases the cost of the binder only 10 percent while its structural coefficient increases 12.5 percent.

4. The superior performance of the three test lanes proves again the efficiency of the pavement section with an interlayer, where a stiff layer of soil cement is covered with a layer of stone, that then has a combination of asphalt base, asphalt binder and asphalt wearing courses applied. This pavement section was very strong, experienced rutting primarily in the wearing and binder courses, and experienced no reflection cracking from the soil cement layer during the two- year observation.

RECOMMENDATIONS

The performance of the test sections in experiment 2 demonstrates the superior nature of a pavement section with a stiff layer at the bottom, a granular interlayer on the stiff layer, and a hot mix asphalt surface. This type of section is similar to that used in Europe where thick, very stiff bases are covered with fairly thin asphalt layers. These European sections have strong, high modulus bases that are designed to be the primary load carrying member, and the thin surfaces are milled and replaced once they become distressed, rough, or slick. The experiment 2 sections also have many of the characteristics of perpetual pavements [*42*] with:

1. Hot mix asphalt characterized as durable and strain-tolerant, and low voids (asphalt content at design plus 0.5 percent) in order to reduce fatigue cracking,

2. A pavement cross section with a strong, high modulus base in order to reduce the strain at the bottom of the hot mix asphalt layer, and

3. A thin wearing course layer that can be milled and replaced to restore ride quality or friction.

The needed hot mix asphalt properties can be achieved using either polymer modified asphalt binders or powdered rubber modified (PRM) asphalt binders, as demonstrated by test results from experiment 2. These elastic modifiers, either polymers or powdered rubber, produce HMA with both high modulus and high strain tolerance when compared to HMA made with conventional asphalt binders. These superior properties are produced at a cost that is only about 10 percent more than that of conventional asphalt binders. The results of experiment 2 prove that the use of these elastic modified binders should be extended to the asphalt base position as demonstrated by the superior performance of lane 2-2 compared to the performance of the conventional design in lane 2-3. As a result of these assessments, the following recommendations are offered to the Department of Transportation and Development:

1. Extend the use of polymer or powdered rubber modified asphalt to all hot mix asphalt pavement layers.

2. Increase the layer coefficient for asphalt bases with modified asphalt and meeting binder course gradations from 0.4 to 0.45.

3. Continue to use a granular base interlayer between the soil cement base and asphalt layers to minimize reflection cracking and extend the fatigue life and rutting resistance of these sections.

4. Continue to use FLEXPASS and ABAQUS as modeling tools to predict the performance and analyze the stress state of flexible pavements tested at the ALF site and to extend the application of those results across Louisiana.

REFERENCES

1. PUBLIC LAW, *Intermodal Surface Transportation Efficiency Act of 1991*, Public Law 102-204, Government Printing Office, Washington, D.C., Dec.18, 1991.

2. "ISTEA Section 1038 and Section 325 of HR 2750", Memorandum from Executive Director, Federal Highway Administration, Department of Transportation, Washington, D.C., November 2, 1993.

3. Heitzman, M., *State of the Practice- Design and Construction of Asphalt Paving Materials with Crumb Rubber Modifier,* Research Report No. FHWA-SA-92-022 Federal Highway Administration, May 1992.

4. Masters, M.F., *Cost Comparisons Using Conventional Methods of Rehabilitation versus Methods using Asphalt-Rubber Systems,* Asphalt Rubber Producers Group National Seminar on Asphalt Rubber, Federal Highway Administration, Department of Transportation, Washington, D.C., 1989.

5. Brown, E.R., *Historical Development,* Crumb Rubber Modifier Workshop Notes, Design Procedures and Construction Practices, Federal Highway Administration, Department of Transportation, Washington, D.C., 1992.

6. Hoyt, D., Lytton, R.L., and Roberts, F.L., *Criteria for Asphalt-Rubber Concrete in Civil Airport Pavements: Evaluation of Asphalt-Rubber Concrete,* Texas Transportation Institute Research Report 4982-2, Federal Aviation Administration, Department of Transportation, Washington, D.C., November 1986.

7. Page, G., *Florida's Initial Experience Utilizing Ground Tire Rubber in Asphalt Concrete Mixes,* Research Report FL/DOT/MO89-366, Florida Department of Transportation, Materials Office, Tallahassee, Fl., September 1989.

8. Maupin, G., Jr., *Hot Mix Asphalt Rubber Applications in Virginia,* Transportation Research Record 1530, Transportation Research Board, Washington, D.C., 1996.

9. Troy, K., Sebaaly, P.E. and Epps, J.A., *Evaluation Systems for Crumb Rubber Modified Binders and Mixtures,* Transportation Research Record 1530,

Transportation Research Board, Washington, D.C., 1996, pp. 3-10.

10. King, W.M., and Abadie, C., *Comparative Performance of Conventional and Rubberized Hot Mix under Accelerated Loading, Construction Report,* FHWA/LA-99/331, Louisiana Transportation Research Center, Louisiana Department of Transportation, Baton Rouge, La., 1999.

11. Statton, J.E., and Kadar, K., *The Performance of Pavement Rehabiliations Under Accelerated Loading – The Callinton ALF Trial,* Proceedings, 15th ARRB Conference Part 2, Australia, 1992.

12. Bonaquist, R., Surdahl, R. and Modawer, W., *Effect of Tire Pressure on Flexible Pavement Response and Performance,* Transportation Research Record 1227, Transportation Research Board, Washington, D.C. 1989.

13. Sebaaley, P., Tabatabaee, N., Bonaquist, R., Avderson, D.A., and Churilla, C. *Pavement Testing Facility - Pavement Performance of the Initial Two Test Sections,* Research Report No. FHWA-RD-88-060, FHWA, U.S. Department of Transportation, Washington, D.C., 1989.

14. Cumbaa, S.L., et al. *Construction and Comparision of Louisiana's Conventional and Alternative Base Courses Under Accelerated Loading*, Research Study, Federal Highway Administration, Washington D.C., 1993 - 1996.

15. Metcalf, J.B., Romanoschie, S., and Li, Y., *Construction and Comparison of Louisiana's Conventional and Alternative Bases under Accelerated Loading, Interim Report 1, Phase 1,* Louisiana Transportation Research Center, Louisiana Department of Transportation and Development, Baton Rouge, La., 1998.

16. Metcalf, J.B., Romanoschie, S., and Li, Y., *The Louisiana Accelerated Loading Facility. Report 2, Experiment 1, Phase 3,* Louisiana Transportation Research Center, Louisiana Department of Transportation and Development, Baton Rouge, La., 1988.

17. Djakfar, L. *Implementation of ALF Results to Designing Flexible Pavements in Louisiana,* A Dissertation for the Degree Doctor of Engineering, Louisiana Tech University, Ruston, La., April 1999.

18. White, T.D., *Application of Finite Element Analysis to Pavement Problems,* Finite Element for Pavement Analysis and Design, Proceedings of the First National Symposium on 3D Finite Element Modeling for Pavement Analysis and Design, Charleston, W.Va., November, 1998.

19. Kenis, W.J. *Predictive Design Procedures, VESYS User Manual - An Interim Design Method for Flexible Pavements Using VESYS Structural Subsystem,* FHWA-RD-77-154, Federal Highway Administration, Department of Transportation, Washington, D.C., January 1978.

20. Lytton, R. L., and Tseng, K.H., *Fatigue Damage Properties of Asphaltic Concrete Pavements*, Transportation Research Record 1286, Transportation Research Board, Washington, D.C., 1990.

21. Zaghloul, S.M., *Non-linear Dynamic Analysis of Flexible and Rigid Pavements* Ph.D. Dissertation, Purdue University, Lafayette, In., 1993.

22. Wathugala, W., Huang, B., and Pal, S., *Numerical Simulation of Geosynthetic-Reinforced Flexible Pavement*, Transportation Research Record 1534, Transportation Research Board, Washington, D.C. 1996.

23. Daly, W. H., and Negulescu, I., *Characterization of Asphalt Cements Modified With Crumbed Rubber from Discarded Tires,* Research Report FHWA/LA-95/291, Louisiana Transportation Research Center, Baton Rouge, LA 1994.

24. Soban, K., Jesick, M., Dedominicis, E., McFadden, J., Cooper, K., and Roe, J., *A Soil-Cement-Fly Ash Pavement Base Course Reinforced with Recycle Plastic Fibers*, 78th Annual Meeting, Transportation Research Board, Washington, D.C., January, 1999.

25. Mohammad, L.N., and Paul, H.R., *Evaluation of the Indirect Tensile Test for Determining the Structural Properties of Asphalt Mix,* Transportation Research Record 1417, Transportation Research Board, Washington, D.C., 1993, pp. 58-63.

26. TexDOT, *Test Method Tex-321-F,* Texas Department of Transportation, Division of Materials and Tests, Austin, Tx., Revised February, 1993.

27. Mohammad, L.N., Zhang, X., Huang, B., and Tan, Z., *Laboratory Performance Evaluation of SMA, CMHB, and Dense Graded Asphalt Mixtures,* Journal of the Asphalt Paving Technologists, Vol. 68, 1999, pp. 252-283.

28. Sousa, J., Solaimanian, M., and Weissman, S., *Development and Use of the Repeated Shear Test (Constant Height): An Optional Superpave Mix Design Tool*, SHRP-A-698, Strategic Highway Research Program, National Research Council, Washington, D.C., 1994.

29. Hua, J., *Finite Element Modeling and Analysis of Accelerated Pavement Testing Devices and Rutting Phenomenon,* Ph.D. Dissertation, Purdue University, Lafayette, IN,2000.

30. HKS, *ABAQUS User's Manual, Version 5.8*, Hibbit, Karlsson & Sorensen, Inc., Pawtucket, RI, 1998.

31. Fernando, E.G., Tseng, K.H., Lytton, R.L., *Flexible Pavement Analysis Structural System (FLEXPASS Release 2.0), User's Guide.* Texas Transportation Institute, Texas A&M University, October, 1989.

32. Duncan, J.M., Monismith, C.L., and Wilson, E.L., *Finite Element Analysis of Pavements,* Highway Research Record 228, Highway Research Board, Washington, D.C., 1968, pp. 18-33.

33. Construction Engineering Laboratory and Facilities Group, *ILLIPAVE-A Finite Element Program for the Analysis of Pavements*. Department of Civil Engineering, University of Illinois at Urbana, May 1982.

34. Tseng, K.H., *A Finite Element Method for the Performance Analysis of Flexible Pavement.* Ph.D. Dissertation. Texas A&M University, College Station. 1988.

35. Huang, B., *Fundamental Characterization and Numerical Analysis of Large Stone Asphalt Mixture,* Ph.D. Dissertation. Louisiana State University, Baton Rouge, La., 2000.

36. Little, D.N., Al-Balbissi, A.H., Gregory, C., and Richey, B., *Design and Characterization of Paving Mixtures Based on Plasticized Sulfur Binders-Engineering Characterization,* Texas Transportation Institute, Draft Final Report, RF 4247, Texas A & M University, College Station, TX, July 1984.

37. Monismith, C.L., *Flexibility Characteristics of Asphalt Pavement Mixtures,* Proceedings, Association of Asphalt Paving Technologists, Vol. 27, 1958, p. 74.

38. Rohde, G.T., *Determining Pavement Structural Number from FWD Testing,* Transportation Research Record 1448, Transportation Research Board, Washington, D.C., 1994, pp.61-68.

39. Irwin, L. H., *User's Guide to MODCOMP2, Version 2.1,* Local Roads Program, Cornell University, Ithica, NY, 1983.

40. Mohammad, L., Huang, B., Roberts, F., and Rasoulian, M., *Accelerated Loading Performance and Laboratory Characterization of Crumb Rubber Asphalt Pavements*, Road Materials and Pavement Design, Volume 1-No. 4/2000, pp. 467-493.

41. Qin, H., *Comparative Performance of Rubberized Hot Mix Asphalt Under ALF Loading,* A Dissertation for the Degree Doctor of Engineering, Louisiana Tech University, Ruston, La., December 2001.

42. *Perpetual Bituminous Pavements,* Transportation Research Circular No. 503, Transportation Research Board, Washington, D.C., December 2001.